APPENDIX 3.9.3
NUHOMS® EOS SYSTEM ACCIDENT DROP EVALUATION

Table of Contents

List of Figures

Proprietary Information on Pages 3.9.3-1 through 3.9.3-13
Withheld Pursuant to 10 CFR 2.390

Figure 3.9.3-8
DELETED

Proprietary Information on Pages 3.9.3-15 and 3.9.3-16
Withheld Pursuant to 10 CFR 2.390

Figure 3.9.3-11
DELETED

Figure 3.9.3-12
DELETED

Figure 3.9.3-13
DELETED

Figure 3.9.3-14
DELETED

Figure 3.9.3-15
DELETED

Figure 3.9.3-16
DELETED

Proprietary Information on This Page
Withheld Pursuant to 10 CFR 2.390

Figure 3.9.3-18
DELETED

Proprietary Information on This Page
Withheld Pursuant to 10 CFR 2.390

APPENDIX 3.9.4
EOS-HSM STRUCTURAL ANALYSIS

Table of Contents

List of Tables

List of Figures

3.9.4 EOS-HSM STRUCTURAL ANALYSIS

The purpose of this appendix is to present the structural evaluation of the EOS-HSM due to all applied loads during storage, loading and unloading operation. The NUHOMS® EOS System consists of the dual-purpose (transportation and storage) EOS-37PTH and EOS-89BTH dry shielded canister (DSC), a horizontal storage module (EOS-HSM), an onsite transfer cask (EOS-TC), and associated ancillary equipment.

3.9.4.1 General Description

General description and operational features for the NUHOMS® EOS System is provided in Chapter 1. The EOS-HSM is a freestanding, reinforced concrete structure, designed to provide environmental protection and radiological shielding for the EOS-37PTH DSC or EOS-89BTH DSC. The drawings of the EOS-HSM, showing different components and overall dimensions, are provided in Chapter 1.

The EOS-HSM consists of a base unit and a roof unit. The roof unit rests mainly on the front and rear walls, and partly on the side walls of the base unit. The roof and the base are connected by bolts/embedments to form a single module via four steel brackets located at each of the interior upper corners of base unit.

An alternate multi-segment design of horizontal storage module, the EOS-HSMS, may also be used in lieu of EOS-HSM as a part of NUHOMS® EOS System. The EOS-HSMS consists of two segments of the base unit and a roof unit. The two segments of base unit of EOS-HSMS are connected by grouted, high-strength, threaded bars/embedments, and the base and roof are connected in a similar way to that of EOS-HSM. EOS-HSM is used herein for both EOS-HSM and EOS-HSMS, unless a unique situation is presented.

The EOS-HSM storage modules can be arranged either in a single-row array, or in back-to-back double-row arrays by placing a module next to, and in contact with, adjacent module(s) with thick end shield walls connected to the EOS-HSM at the end of the arrays. The thick rear shield walls are also connected to the back wall of the EOS-HSM, if the modules are placed in a single-row array.

The EOS-37PTH DSC or EOS-89BTH DSC is supported inside the EOS-HSM by DSC support structure. The DSC support structure is comprised of two main support beams, two extension plates and two nitronic sliding rails and it spans between the front wall and the rear wall of the base unit. The web of the main support beams has openings to allow the air flow around the DSC. The DSC support structure provides support for the DSC during storage and also acts as a sliding surface during the insertion and retrieval of DSC.

The width of EOS-HSM is 116 inches. The overall height of EOS-HSM is 240 inches including the outlet vent cover. Three different EOS-HSM lengths are available in order to accommodate DSCs of different lengths. The internal cavity of the EOS-HSM accommodates DSCs of variable length by varying the location of the axial retainer and by variation of gap between the DSC and the EOS-HSM back wall.

The air inlet vents located at the front lower corners of base unit extend through the bottom of side wall on both sides, which ultimately lead to the cavity of base unit. The air outlet vents are provided in the roof at both sides of the module.

The front wall of EOS-HSM base unit has round access door opening provided for transferring EOS-37PTH DSC or EOS-89BTH DSC into the module or retrieving it from the module. The door opening is closed by a shield door after the insertion of EOS-37PTH DSC or EOS-89BTH DSC. The EOS-HSM shield door is a combination of rectangular and cylindrical concrete block with steel backing plate on the inside face. The shield door provides environmental protection, including missile and shielding protection.

End shield walls are installed at each end of a module array to provide the required missile and shielding protection. Similarly, a rear shield wall is installed at the rear of each module of the single row module array for same purpose.

For thermal protection of the EOS-HSM concrete, a thin stainless steel heat shield is installed inside the EOS-HSM. The interior surface of the upper part of the side wall is protected with side heat shields, and the underside of the roof unit is protected with a roof heat shield. The roof heat shield has an upward slope at 10 degrees from center towards outlet vent. The heat shield guides the cooling air flow through the EOS-HSM.

During DSC insertion and retrieval operations, the EOS-TC is docked with the EOS-HSM docking surface and mechanically secured to the cask restraint embedments provided in the front wall of the base unit. These embedments are equally spaced on either side of the door opening and located near the lower embedment for door attachment.

3.9.4.2 Material Properties

The material properties used in the analysis and design of EOS-HSM and its components are discussed in detail in Chapter 8.

3.9.4.3 Design Criteria

The reinforced concrete EOS-HSM and the DSC support structure are important to safety components of NUHOMS® EOS System. Consequently, they are designed and analyzed to perform their intended functions under the extreme environmental and natural phenomena specified in 10 CFR 72.122 [3.9.4-1] and American National Standards Institute (ANSI) 57.9 [3.9.4-10]. These include tornado and wind, seismic, and flood design criteria. The design wind pressure is determined as per American Society of Civil Engineers (ASCE) 7-10 [3.9.4-15].

The concrete EOS-HSM and steel DSC support structures are designed to the requirements of American Concrete Institute (ACI) 349-06 [3.9.4-12] and the American Institute of Steel Construction (AISC) Manual of Steel Construction [3.9.4-14], respectively, using the load combinations prescribed by ANSI 57.9 [3.9.4-10]. When ACI-349-06 does not have enough information, ACI-318-08 [3.9.4-11] is used as supplement. The following table summarizes the Codes and Standards for design and fabrication of these components.

Component	Material	Applicable Code
EOS-HSM Concrete Components	Concrete	ACI 349-06 (Design) ACI 318-08 (Fabrication) ASCE 7-10 (Loads) ANSI/ANS 57.9-84 (Loads & Load Combination)
DSC Support Structure, Heat Shields and other Steel Components	Steel	AISC Manual of Steel Construction,13th Edition (Structural Steel) AWS D1.1, March 2010 (Structural Weld) ASCE 7-10 (Loads) ANSI/ANS 57.9-84 (Loads & Load Combination)

The ultimate strength method of ACI 349-06 [3.9.4-12] is used for the design of the EOS-HSM reinforced concrete structural components. The reinforcement is provided to meet the minimum flexural and shear reinforcement requirement of ACI 349-06 and to ensure that the provided design strength exceeds the required strength. Alternatively, for some cases, the minimum reinforcement area requirement can be waived for components with a flexural stress ratio of less than 0.66 as per Section 10.5.3 of ACI 349-06 [3.9.4-12].

The axial, shear and moment capacities for all the concrete components of the EOS-HSM calculated based on ACI 349-06 are provided in Table 3.9.4-11 and Table 3.9.4-12. The capacities for blocked vent accident condition consider the strength reduction at elevated temperature.

The required steel strength, S, and required steel shear strength, S_v, for critical section of steel structure are calculated in accordance with the requirements of AISC Steel Construction Manual [3.9.4-14] using the Allowable Strength Design (ASD) method.

3.9.4.4 Load Cases

A summary of the design loads for EOS-HSM concrete component evaluation is provided in Table 3.9.4-4. This table also presents the applicable codes and standards for specific load. A summary of the design loads for DSC support structure is provided in Table 3.9.4-15.

3.9.4.5 Load Combination

The load combinations used in the structural analysis of EOS-HSM and DSC support structure comply with the requirement of 10 CFR 72.122 [3.9.4-1] and ANSI 57.9-84 [3.9.4-10]. Table 3.9.4-5 and Table 3.9.4-16 summarize the load combination requirement of EOS-HSM and DSC support structure, respectively.

3.9.4.6 Finite Element Models

EOS-HSM has variable length to store the DSCs of different lengths, however, only the longest module (EOS-HSM Long) is analyzed since it governs the structural design.

3.9.4.6.1 Finite Element Model to Evaluate EOS-HSM Concrete Components for Mechanical Loads

The structural analysis of an individual module provides a conservative estimate of the response of the EOS-HSM structural elements under the postulated static and dynamic loads for any EOS-HSM array configuration. The frame and shear wall action of the EOS-HSM concrete components are considered to be the primary structural system resisting the loads. The analytical model is evaluated for normal operating, off-normal, and postulated accident loads acting on the EOS-HSM.

A three-dimensional (3D) ANSYS finite element model (FEM) of the EOS-HSM, including all the concrete components, is developed. The eight-node brick element (ANSYS element type SOLID185) is used to model the concrete structure. Each node of the eight-node brick element has three translational degrees of freedom. The DSC is modeled using beam elements (ANSYS element type BEAM4). The DSC main support beam, W12x136 and the brace, C3x5 are also modelled using beam elements with appropriate section properties. The mass of the DSC is lumped at eleven discrete nodes of the beam using lumped mass elements (ANSYS element type MASS21). A plot of the ANSYS model of EOS-HSM and EOS-HSMS is shown in Figure 3.9.4-1 and Figure 3.9.4-2, respectively.

The DSC support structure is incorporated into the EOS-HSM analytical model to transfer the load to concrete components. The connections of the support structure to the concrete structure are modeled using rigid beam elements. The various normal, off-normal and accident loads are applied to the analytical model and internal forces and moments are computed by performing a linear elastic finite element analysis.

The node coupling option of ANSYS is used to represent the appropriate connection between the base and roof of the EOS-HSM model. For EOS-HSMS, the node to node contact element (ANSYS element type CONTA178) is used across the interface of the upper and lower segment to transfer the load from the roof and upper segment to the lower segment. The counter bore and rail extension baseplate groove at the door opening are not included in the FEM. Conservatively, the nodes at the bottom of EOS-HSM are constrained in all three translational degree of freedom, thus maximizing the EOS-HSM design forces and moments.

3.9.4.6.2 Finite Element Model of the EOS-HSM Concrete Structure for Thermal Stress Analysis

Thermal stress analyses of the EOS-HSM were performed using a 3D FEM, which includes only the concrete components. The connections of the door and the support structure rails to the EOS-HSM concrete structure are designed so that free thermal growth is permitted in these members when the EOS-HSM is subjected to thermal loads. Because of their free thermal growth, the door and the support structure do not induce thermal stresses in the concrete components of the EOS-HSM. Therefore, the analytical model of the EOS-HSM for thermal stress analysis of the concrete components does not include the DSC support structure and the door. The ANSYS models with temperature profile, which is used to perform thermal stress analysis of the concrete components, are shown in Figure 3.9.4-3 and Figure 3.9.4-4.

For the thermal load analysis, the bottom of the EOS-HSM (y=0 in ANSYS model) was restrained at one set of edge nodes (in axial and lateral directions) and friction forces were applied at the bottom of EOS-HSM base in the axial and lateral directions. One node in the front wall and two nodes in the back wall at y=0 are also restrained in vertical direction.

3.9.4.6.3 Finite Element Model for Structural Analysis of DSC Support Structure

A 3D FEM of the DSC main support beam with stiffener plates and rail extension baseplate is developed in the computer program ANSYS [3.9.4-19]. In the finite element model (FEM) for the DSC main support beam (W12x136), the W section of the main support beam is broken down into flange and web components represented individually by BEAM189 elements.

The beam elements (BEAM189) are arranged in a 2D plane aligned with the centerline of the beam, inclined 30 degrees from vertical along the length of the beam. Each element has three nodes with six degrees of freedom (three translational and three rotational) per node.

The web of the DSC main support beam has triangular openings, allowing for heat flow, resulting in vertical and diagonal web elements. The cross sections of these components are calculated and used to define the assigned cross sections for each component. A plot of the front portion of the model of the DSC main support beam model is shown in Figure 3.9.4-6.

The model is completely restrained at the bottom end of the rail extension baseplate. The ends of the DSC main support beam at the bottom are restrained for vertical displacement and rotation about longitudinal axis to simulate the simple support condition of the concrete pedestals at the front and rear walls. The support beam is also restrained laterally at the location of lateral braces.

The ETAB command of ANSYS is used to extract the beam element results due to individual load cases which then combined to determine the combined load results.

3.9.4.6.4 Finite Element Model for Structural Analysis of Heat Shield Panels and Connection Studs

The heat shields (coupled panel-stud system) are subjected to two loads: a combination of 1g dead load due to its own weight, and a seismic load that is dependent upon its natural frequency as well as the in-structure response spectra (ISRS) at the supports of the plate-stud system.

Modal time-history analysis of the EOS-HSM is performed using ANSYS computer code to determine the ISRS at the nodes at which the studs are supported. Applicable time-histories and modal properties for this evaluation are provided in Section 3.9.4.9.2.

ANSYS is also used to determine the natural vibration frequencies of the coupled panel-stud system. Shell elements (ANSYS element type SHELL63) are used to model the heat shield panel and beam elements (ANSYS element type BEAM4) are used for the studs. The FEM of the coupled panel-stud system is shown in Figure 3.9.4-8 and Figure 3.9.4-9.

The natural frequency of the plate-stud system is used to determine the appropriate g load from the ISRS. It is assumed that the heat shields are dynamically decoupled from the EOS-HSM because the concrete EOS-HSM is much more rigid than the heat shields and the weight of the heat shield is small as compared to the total weight of loaded EOS-HSM. Accordingly, the heat shields are not accounted for in the modal time-history analysis of the EOS-HSM, and the EOS-HSM is not considered in modal analysis of the heat shields.

3.9.4.7 Normal Operation Structural Analysis

The evaluation of the EOS-HSM is performed at normal operating condition. The following table shows the normal operating loads for which the EOS-HSM components are designed. The table also lists the individual EOS-HSM components that are affected by each loading.

Load Type	Components	
	EOS-HSM	**DSC Support Structure**
Dead Load	X	X
Live Load	X	X
Normal Handling	X	X
Normal Thermal	X	X
Wind Load	X	

The reinforced concrete and the steel DSC support structure of the EOS-HSM are analyzed for the normal, off-normal, and postulated accident conditions using FEMs described in Section 3.9.4.6. These models are used to evaluate concrete and support structure forces and moments due to dead load, live load, normal handling loads, normal thermal loads, and wind load. The methodology used to evaluate the effects of these normal loads is addressed in the following paragraphs.

3.9.4.7.1 EOS-HSM Dead Load (DL) Analysis

Dead loads are applied to the analytical model by application of 1g acceleration in the vertical direction where g is the gravitational acceleration (386.4 in/sec2). The 5% variation of dead load as indicated in ANSI/ANS 57.9 is not used because the heaviest design weight is used for analysis.

3.9.4.7.2 EOS-HSM Live load (LL) Analysis

Live load analysis is performed by applying 200 psf pressure on the roof. The DSC weight is also applied on the DSC support structure as a live load.

3.9.4.7.3 EOS-HSM Normal Operational Handling Load (R_o) Analysis

Normal operation assumes the canister is sliding over the DSC support structure due to a hydraulic ram force of up to 135,000 lbs (insertion) and 80,000 lbs (extraction) applied at the grapple ring. The normal operation handling load of 70,000 lbs is applied to each DSC main support beam in the axial direction resulting in a total applied load of 140,000 lbs on both beams which conservatively envelopes the total insertion/extraction force. The same magnitude of load of 70,000 lbs is also applied at each of the cask restraint embedment in opposite direction. In addition, the DSC weight is applied as a distributed load on both DSC support beam of the EOS-HSM.

3.9.4.7.4 EOS-HSM Normal Operating Thermal (T_o) Stress Analysis

The normal operating thermal (T_o) loads on EOS-HSM include the effect of design basis heat load up to 50 kW generated by DSC, plus the effect of normal ambient temperature range. To evaluate the effects of normal thermal loads on the EOS-HSM, heat transfer analyses for a range of normal ambient temperatures (-20 °F and 100 °F) are performed with DSC heat load of 50 kW. The normal thermal cold condition (-20 °F) is bounded by off-normal thermal cold condition (-40 °F). Therefore, off-normal thermal cold condition is used in place of normal thermal cold condition. The ambient condition that causes maximum temperature and maximum gradients in the concrete components is used in the analysis. The normal thermal hot condition is the governing case for this load case. The EOS-HSM thermal stress analysis was performed using thermal profiles and maximum temperatures that bounds those reported in Chapter 4.

3.9.4.7.5 EOS-HSM Design Basis Wind Load (W) Analysis

The DSC support structure and DSC inside the EOS-HSM are not affected by wind load. The concrete structure forces and moments due to design basis wind load (W) are bounded by the result of tornado generated wind load discussed in Section 3.9.4.9.1. Therefore, tornado generated wind load is conservatively used in the off-normal wind load combination C2, as seen in Table 3.9.4-5. Therefore, no separate analysis is performed for the design basis wind load case.

3.9.4.8 Off-Normal Operation Structural Analysis

This section describes the design basis off-normal events for the EOS-HSM components and presents analyses that demonstrate the adequacy of the design safety features of the EOS-HSM.

The following table shows the off-normal operating loads for which the EOS-HSM components are designed.

	Components	
Load Type	**EOS-HSM**	**DSC Support Structure**
Off-Normal Handling	X	X
Off-Normal Thermal	X	X

For an operating NUHOMS® EOS System, off-normal events could occur during fuel loading, TC handling, canister transfer, trailer towing, and other operational events. Two credible off-normal events as listed in the above table are defined that bound the range of off-normal conditions for EOS-HSM. The limiting off-normal events are defined as a jammed DSC during loading or unloading from the EOS-HSM and the extreme ambient temperatures of -40 °F (winter) and +117 °F (summer). These events bound the range of expected off-normal structural loads and off-normal temperatures range acting on the EOS-HSM. ANSYS FEMs described in Section 3.9.4.6 are used to evaluate concrete and support structure forces and moments due to these loads.

3.9.4.8.1 EOS-HSM Off-Normal Handling Loads (Ra) Analysis

This load case assumes that the EOS-TC is not accurately aligned with respect to the EOS-HSM resulting in binding of the DSC during a transfer operation causing the hydraulic pressure in the ram to increase. The ram force is limited to a maximum load of 135,000 lbs during insertion, as well as during retrieval. Therefore, for the DSC support structure, the off-normal jammed canister load (R_a) is defined as an axial load of 135 kips on one DSC support beam, plus a vertical load of one half the DSC weight (on both rails) at the most critical location.

3.9.4.8.2 EOS-HSM Off-Normal Thermal Loads Analysis

This load case is the same as the normal thermal load, but with an ambient temperature range from -40 °F to 117 °F. The temperature distributions for the extreme ambient conditions are used in the analysis for the concrete component evaluation.

3.9.4.9 Accident Condition Structural Analysis

The design basis accident events specified by ANSI/ANS 57.9-1984, and other credible accidents postulated to affect the normal safe operation of the EOS-HSM are addressed in this section.

Each accident condition is analyzed to demonstrate that the requirements of 10 CFR 72.122 are met and that adequate safety margins exist for the EOS-HSM design. The resulting accident condition stresses in the EOS-HSM components are evaluated and compared with the applicable code limits. The postulated accident conditions addressed in this section include:

- Tornado winds and tornado generated missiles (W_t, W_m)
- Design basis earthquake (E)
- Design basis flood (FL)
- Blocked Vent Accident Thermal (T_a)

ANSYS FEMs described in Section 3.9.4.6 are used to evaluate concrete and support structure forces and moments due to these loads.

3.9.4.9.1 Tornado Winds/Tornado Missile Load (W_t, W_m) Analysis

The most severe tornado generated wind and missile loads selected for analysis specified by NRC Regulatory Guide 1.76 [3.9.4-4] and NUREG-0800 [3.9.4-7]. The extreme design basis wind loads are less severe than tornado generated wind loads and, therefore, do not need to be addressed.

The tornado wind intensities used for the EOS-HSM analysis are obtained from NRC Regulatory Guide 1.76, Rev. 0 [3.9.4-4], which bound the design basis requirements. Region I intensities are utilized since they result in the most severe loading parameters. For this region, the maximum wind speed is 360 mph, the rotational speed is 290 mph, and the maximum translational speed is 70 mph. The radius of the maximum rotational speed is 150 ft, the pressure drop across the tornado is 3 psi and the rate of pressure drop is 2 psi per second [3.9.4-4].

The maximum wind speed used of 360 mph provides substantial conservatism relative to the maximum wind speed of 230 mph prescribed in current regulatory guidance in NRC Regulatory Guide 1.76 Revision 1 [3.9.4-22]. For the purposes of the structural evaluation as described in Chapter 3 and its associated appendices, as well as the accident evaluation as described in Chapter 12 the design basis tornado (DBT) refers to the bounding criteria from Regulatory Guide 1.76, Rev. 0 used in the analysis.

Tornado loads are generated for three separate loading phenomena:

- Pressure or suction forces created by drag as air impinges and flows past the EOS-HSM. These pressure or suction forces are due to tornado generated wind with maximum wind speed of 360 mph.
- Pressure or suction forces created by drag due to tornado generated pressure drop or differential pressure load of 3 psi.
- Impact, penetration and spalling forces created by tornado-generated missiles impinging on the EOS-HSM.

The determination of impact forces created by tornado missiles for the EOS-HSM is consistent with that presented in Section 2.3.1.2. The four types of missiles listed below envelope the missile spectrum of NUREG-0800, Revision 2, Section 3.5.1.4 [3.9.4-7]. These missiles also bound the design basis missile spectrum of NRC Regulatory Guide 1.76, Revision 1 [3.9.4-22] and NUREG 0800, Revision 3, Section 3.5.1.4 [3.9.4-8]. Evaluation of the effects of small diameter spherical missiles (artillery) is not required because there are no openings in the EOS-HSM leading directly to the DSC through which such missiles could pass.

1. Utility wooden pole, 13.5" diameter, 35' long, Weight = 1500 lbs, Impact velocity = 294 fps.

2. Armor piercing artillery shell 8" diameter, Weight = 276 lbs, Impact velocity = 185 fps.

3. Steel pipe, 12" diameter, Schedule 40, 30 ft long, Weight = 1500 lbs, Impact velocity = 205 fps.

4. Automobile traveling through the air not more than 25 ft above the ground and having contact area of 20 sq. ft, Weight = 4000 lbs, Impact Horizontal Velocity = 195 fps.

Stability and stress analyses are performed to determine the response of the EOS-HSM to tornado wind pressure loads. The stability analyses are discussed in detail in Appendix 3.9.7. The stress analyses are performed using the ANSYS FEM of a single EOS-HSM to determine design forces and moments. These conservative analyses envelope the effects of wind pressures on the EOS-HSM array. Thus, the requirements of 10 CFR 72.122 are met.

The EOS-HSM is qualified for maximum design basis tornado (DBT) generated design wind loads of 218 psf and 154 psf on the windward and leeward EOS-HSM walls (See Table 3.9.4-1 and Table 3.9.4-2), and a pressure drop of 3 psi.

A single, stand-alone EOS-HSM is protected by shield walls, or an adjacent module on either side and at the rear. For an EOS-HSM array, the critical module is on the windward end of the array. This module has an end shield wall to protect the module from tornado missile impacts. The shield wall is also subjected to the 218 psf windward pressure load. The leeward side of the same end module in the array has no appreciable suction load due to the presence of the adjacent module. The 154 psf suction load is applicable to the end shield wall on the opposite end module in the array. A suction of 326 psf is also applied to the roof of each EOS-HSM in the array.

For the stress analyses, the DBT wind pressures are applied to the EOS-HSM as uniformly distributed loads. The rigidity of the EOS-HSM in the transverse direction, due to frame and shear wall action of the EOS-HSM, is the primary load transfer mechanism assumed in the analysis. The bending moments and shear forces at critical locations in the EOS-HSM concrete components are calculated by performing an analysis using the ANSYS analytical model of the EOS-HSM as described in Section 3.9.4.6. The resulting moments and forces are included in the EOS-HSM load combination results reported in Table 3.9.4-7 to Table 3.9.4-10.

Conservatively, the design basis extreme wind pressure loads are assumed to be equal to those calculated for the DBT (based on 360 mph wind speed) in the formulation of EOS-HSM load combination results.

In addition, the adequacy of the EOS-HSM to resist tornado missile loads is checked using the modified National Defense Research Committee (NDRC) empirical formulae [3.9.4-13] for local damage evaluation, and response chart solution method [3.9.4-18] for global response. These evaluations are described in Section 3.9.4.10.6.

3.9.4.9.2 Earthquake (Seismic) Load (E) Analysis

The design basis seismic load used for analysis of the EOS-HSM components is as discussed in Section 2.3.4. Based on U.S. NRC (NRC) Regulatory Guide 1.61 [3.9.4-3], a damping value of four percent is used for seismic analysis of steel structural components and a damping value of seven percent is used for seismic analysis of concrete components of EOS-HSM. An evaluation of the frequency content of the loaded EOS-HSM is performed to determine the amplified accelerations associated with the design basis seismic response spectra for EOS-HSM.

The design basis accelerations for the EOS-HSM are amplified based on the results of the frequency analysis of the EOS-HSM. The results of the frequency analysis of the EOS-HSM structure (which includes a simplified model of the DSC) yield a lowest frequency of 18.7 Hz in the transverse direction and 32.7 Hz in the longitudinal direction. The lowest vertical frequency exceeds 45 Hz; therefore the spectral acceleration is not amplified in vertical direction. Thus, based on the Regulatory Guide 1.60 response spectra amplifications, and conservatively using ZPA accelerations of 0.50g and 0.33g in the horizontal and vertical directions, respectively, the corresponding seismic accelerations used for the design of the EOS-HSM are 0.936g and 0.628g in the transverse and longitudinal directions, respectively, and 0.333g in the vertical direction. The resulting amplified accelerations are given in Table 3.9.4-3.

An equivalent static analysis of the EOS-HSM is performed using the ANSYS model described in Section 3.9.4.6 by applying the amplified seismic accelerations load. These amplified accelerations are determined based on the frequency analysis of the EOS-HSM. The frequency analysis of EOS-HSM and multi-segment design EOS-HSMS was performed individually and found that EOS-HSMS yields bounding amplified acceleration. Therefore, the bounding amplified acceleration derived from modal analysis of EOS-HSMS is conservatively used for both EOS-HSM and EOS-HSMS.

The responses for each orthogonal direction are combined using the square root of the sum of the squares (SRSS) method. The resulting moments and forces due to combined seismic load are included in the EOS-HSM load combination results.

For sites where the response spectra at the base of the HSM are larger than analyzed, more than one module may need to tie together to prevent significant sliding or to prevent the modules from banging into each other causing unacceptable damage. The reinforcement requirement may also need to be reviewed, and additional rebar may be added for such sites.

The stability evaluation of the EOS-HSM due to a 0.45g Horizontal/0.30g Vertical seismic load is discussed in Appendix 3.9.7.

For dynamic analysis, the stability evaluation shall be performed using the analysis methodology described in CoC 1029 [3.9.4-21].

Seismic analysis of the EOS-HSM heat shields consists of a modal time-history analysis of the EOS-HSM for obtaining the ISRS at heat shields support locations and an equivalent static analysis of the EOS-HSM heat shields using the seismic acceleration load corresponding to the ISRS obtained in the first step. The earthquake time histories compatible with the RG 1.60 spectra are used as seismic input motion. The acceleration, velocity, and displacement time histories and corresponding spectra of the motion in the two horizontal and vertical directions, all with 1.0g ZPA, are shown in Figure 3.9.4-10 through Figure 3.9.4-15. The ISRS of the side heat shield support nodes are shown in Figure 3.9.4-10, Figure 3.9.4-11, and Figure 3.9.4-12. Modal frequencies and mass participation factors of the EOS-HSMS3 are shown in Table 3.9.4-23. From the modal time-history analysis, the ISRS with a damping value of four percent are obtained at the support locations of the heat shields are shown in Figure 3.9.4-16 through Figure 3.9.4-21. Modal participations factors for the roof heat shield and side heat shield are shown in Table 3.9.4-24 and Table 3.9.4-25, respectively. The ISRS for the head heat shields is conservatively determined using ground motion based on the RG 1.60 spectra anchored at 0.50g and 0.33g in the horizontal and vertical directions, respectively.

3.9.4.9.3 Flood Load (FL) Analysis

Since the source of flooding is site specific, the exact source, or quantity of flood water, should be established by the licensee. However, for this generic evaluation of the EOS-HSM, bounding flooding conditions are specified that envelope those that are postulated for most plant sites. As described in Section 2.3.3, the design basis flooding load is specified as a 50-foot static head of water and a maximum flow velocity of 15 feet per second. Each licensee should confirm that this represents a bounding design basis for their specific ISFSI site.

Since the EOS-HSM is open to the atmosphere, static differential pressure due to flooding is not a design load.

The maximum drag pressure, D, acting on the EOS-HSM due to a 15 fps flood water velocity is calculated as follows:

$$D = \frac{C_D \rho_w V^2}{2g} \quad [3.9.4\text{-}20]$$

Where:

V = 15 fps, Flood water velocity

C_D = 2.0, Drag coefficient for flat plate

ρ_w = 62.4 lb/ft^3, Flood water density

g = 32.2 ft/sec^2, Acceleration due to gravity

D = Drag pressure (psf)

The resulting flood induced drag pressure is: D = 436 psf.

The following flood load cases are considered to account for different flow direction:

- Case 1: Flood water flow from front to rear of EOS-HSM
- Case 2: Flood water flow from rear to front of EOS-HSM
- Case 3: Flood water flow from right side to left side of EOS-HSM or vice versa

ANSYS FEM described in Section 3.9.4.6 is used for the structural evaluation. The results for flood load case are obtained by enveloping results from above load cases.

The stability evaluation of EOS-HSM due to flood load is discussed in Appendix 3.9.7.

3.9.4.9.4 Accident Blocked Vent Thermal (T_a) Stress Analysis

This accident conservatively postulates the complete blockage of the EOS-HSM ventilation air inlet and outlet openings.

Since the EOS-HSMs are located outdoors; there is a remote probability that the ventilation air inlet and outlet vent openings could become blocked by debris from events such as flooding, high wind and tornados. Design features, such as the perimeter security fence and the redundant protected location of the air inlet, and outlet vent openings and the screens reduce the probability of occurrence of such an accident. Nevertheless, for this conservative generic analysis, such an accident is postulated to occur and is analyzed.

The postulated accident thermal event occurs due to blockage of the air inlet and outlet vents under off-normal ambient temperatures range from -40 ºF to 117 ºF.

ANSYS FEM described in Section 3.9.4.6 is used for the structural analysis for accident blocked vent condition.

3.9.4.10 Structural Evaluation

The load categories associated with normal operating conditions, off-normal conditions and postulated accident conditions are described previously. The load combination results and design strengths of EOS-HSM components are presented in this section.

3.9.4.10.1 EOS-HSM Concrete Components

To determine the required strength (internal axial forces, shear forces, and bending moments) for each EOS-HSM concrete component, linear elastic finite element analyses are performed for the normal, off-normal, and accident loads using the analytical models described in Section 3.9.4.6 for mechanical and thermal loads.

The concrete design loads are multiplied by load factors and combined to simulate the most adverse load conditions. The load combinations listed in Table 3.9.4-5 are used to evaluate the concrete components. The bounding load combination results for each component are presented in Table 3.9.4-7 to Table 3.9.4-10. The notations for the components of forces and moments and the concrete component planes in which capacities are computed are shown in Figure 3.9.4-5. The thermal stresses of EOS-HSM concrete components used in the load combination results are based on thermal results that bound those reported in Chapter 4. All load combination results are less than computed section capacities.

The required strength, U, for critical sections of concrete is calculated in accordance with the requirements of ANSI 57.9 [3.9.4-10] and ACI 349-06 [3.9.4-12], including the strength reduction factors defined in ACI 349-06, Section 9.3. The design strength of EOS-HSM concrete components exceeds the factored design loads. Thus, the EOS-HSM concrete components are adequate to perform their intended function. EOS-HSM construction details such as construction joints and reinforcement bar splices is detailed on the construction drawings.

3.9.4.10.2 DSC Support Structure

The DSC main support beams, stiffener plates, extension baseplates, DSC stop plates and braces members of the DSC support structure are evaluated using the allowable strength design method of the AISC Manual of Steel Construction [3.9.4-14]. The maximum temperature used in the stress analysis of the support steel bounds the maximum temperature reported in Chapter 4.

The load combination results for each of these components are provided in Table 3.9.4-17 to Table 3.9.4-22. The maximum value of demand to capacity ratio of DSC support structure is less than 1.0. Thus, DSC support structure is adequately strong to resist the reasonably foreseeable loads applied to it.

3.9.4.10.3 EOS-HSM Shield Door

The shield door is free to grow in the radial direction when subjected to thermal loads. Therefore, there are no stresses in the door due to thermal growth. The dead weight, tornado wind, differential pressure and flood loads cause insignificant stresses in the door compared to stresses due to missile impact load. Therefore, the door is evaluated only for the missile impact load.

The minimum thickness of concrete component to prevent perforation, and scabbing are 18.5 inches and 27.7 inches, respectively. Thus, the 30.5-inch thick door is adequate to protect from local damage due to missile impact. The computed maximum ductility ratio for the door is less than 1, which satisfies the ductility requirement if compared against the allowable ductility ratio of 10 as per ACI 349-06 [3.9.4-12]. Therefore, the concrete door meets the ductility requirement and is adequate to protect from global effect of missile impact.

For the door anchorage, the controlling load is tornado generated differential pressure drop load. The maximum tensile force per bolt (four door attachment bolts), is 7.6 kips. The design strength of door attachment embedment (nonductile) as per Section D.3.6.3 of ACI 349-06 [3.9.4-12] is 17.99 kips, which is greater than 7.6 kips, thus satisfying the ACI 349-06 code requirement.

3.9.4.10.4 EOS-HSM Heat Shield

The roof heat shield assembly consists of four panels. Each panel section is a v-shaped in transverse direction with v-notch at the center of the EOS-HSM width. The roof heat shield panels are connected to the roof by fifteen, ¾-10UNC bolts. The natural lateral frequency of a typical panel/connection stud system is determined from ANSYS computer code. The maximum interaction ratio for combined axial and bending stress in the connection bolts is 0.503, which is less than 1.0. The maximum bending moment in roof heat shield panel is 22.29 in-lb/in., which is also less than the panel moment capacity of 59.59 in-lb/in.

The side wall heat shield assembly also consists of four panels. The side wall heat shield panels are attached to the EOS-HSM base unit side wall by seventeen ½-13UNC bolts on both sides. The maximum interaction ratio for combined axial and bending stress in connection bolts is 0.563, which is less than 1.0. The maximum bending moment in side heat shield panel is 46.98 in-lb/in, which is also less than the panel moment capacity of 59.59 in-lb/in.

The maximum temperature used in the stress analysis of the heat shields bounds the maximum temperatures reported in Chapter 4. The size of the slot hole provided in the panel at the connection bolt location is sufficiently large to allow for free thermal expansion. Therefore, neither of roof heat shield panel and side wall heat shield panel is subjected to thermal stress.

3.9.4.10.5 EOS-HSM DSC Axial Restraint

The DSC axial restraint consists of a capped steel tube embedment located within the bottom center of the round access opening of the EOS-HSM front wall, and a 2-inch by 4-inch solid bar steel retainer that drops into the embedment cavity after DSC transfer is complete. The drop-in retainer extends approximately 5 inches above the top of embedment to provide axial restraint of the DSC. The maximum seismically induced shear load in the retainer is 140.5 kips. The allowable shear strength of the axial retainer is 196.0 kips. The maximum seismically induced moment in the retainer is 281.0 in-kips taking a moment arm of 2 inches, conservatively. The allowable flexural strength of axial retainer is 344.9 in-kips. Hence, the DSC axial retainer design is adequate to perform its intended function.

3.9.4.10.6 Evaluation of Concrete Components for Missile Loading

Missile impact effects are assessed in terms of local damage and overall structural response. Local damage that occurs in the immediate vicinity of the impact area is assessed in terms of penetration, perforation, spalling and scabbing. Evaluation of local effects is essential to ensure that protected items (the DSC and fuel) would not be damaged by a missile perforating a protective barrier, or by secondary missiles such as scabbing particles. Evaluation of overall structural response is essential to ensure that protected items are not damaged or functionally impaired by deformation or collapse of the impacted structure.

The tornado-generated missiles are conservatively assumed to strike normal to the surface with the long axis of the missile parallel to the line of flight to maximize the local effects. Plastic deformation to absorb the energy input by the tornado-generated missile load is desirable and acceptable, provided that the overall integrity of the structure is not impaired. Due to complex physical process associated with missile impact effects, the EOS-HSM structure is primarily evaluated conservatively by application of empirical formulae.

3.9.4.10.6.1 Local Damage Evaluation

Local missile impact effects consist of (a) missile penetration into the target, (b) missile perforation through the target, and (c) spalling and scabbing of the target. This also includes punching shear in the region of the target. Per F.7.2.3 of ACI 349-06 [3.9.4-12], if the concrete thickness is at least 20% greater than that required to prevent perforation, the punching shear requirement of the code need not be checked.

The following enveloping missiles are considered for local damage:

- Utility wooden pole
- Armor piercing artillery shell
- 12-inch diameter schedule 40 steel pipe

Large deformable missiles such as automobiles are incapable of producing significant local damage. Concrete thickness satisfying the global structural response requirements including punching shear is considered to preclude unacceptable local damage. Therefore, the local effects from an automobile are evaluated using punching shear criteria of ACI 349-06 [3.9.4-12].

The following empirical formulae are used to determine the local damage effects on reinforced concrete target:

B. Modified NDRC formulas for penetration depth [3.9.4-13]:

$$x = \sqrt{4KNWd\left(\frac{v_o}{1000\ d}\right)^{1.8}}\ , \text{ for } x/d \le 2.0$$

$$x = \left[KNW\left(\frac{v_o}{1000\ d}\right)^{1.8}\right] + d\ , \text{ for } x/d > 2.0$$

Where,

x = Missile penetration depth, inches

K= concrete penetrability factor = $\frac{180}{\sqrt{f_c'}}$

N = projectile shape factor
= 0.72 flat nosed
= 0.84 blunt nosed
= 1.0 bullet nosed (spherical end)
= 1.14 very sharp nose

W = weight of missile, lb

v_o = striking velocity of missile, fps

d = effective projectile diameter, inches.
for a solid cylinder, d = diameter of projectile and
for a non-solid cylinder, $d = (4A_c/\pi)^{1/2}$

A_c = projectile impact area, in^2

C. Modified NDRC formula for perforation thickness [3.9.4-13]:

$$\frac{e}{d} = 3.19\left(\frac{x}{d}\right) - 0.718\left(\frac{x}{d}\right)^2 \text{ , for } x/d \le 1.35$$

$$\frac{e}{d} = 1.32 + 1.24\left(\frac{x}{d}\right) \text{ , for } 1.35 \le x/d \le 13.5$$

Where,

e = perforation thickness, in.

In order to provide an adequate margin of safety the design thickness $t_d = 1.2e$ [3.9.4-12]

D. Modified NDRC formula for scabbing thickness [3.9.4-13]:

$$\frac{s}{d} = 7.91\left(\frac{x}{d}\right) - 5.06\left(\frac{x}{d}\right)^2 \text{ , for } x/d \le 0.65$$

$$\frac{s}{d} = 2.12 + 1.36\left(\frac{x}{d}\right) \text{ , for } 0.65 \le x/d \le 11.75$$

Where,

s = scabbing thickness, in.

In order to provide an adequate margin of safety the design thickness td = 1.2s [3.9.4-12]

The concrete targets of the EOS-HSM that may be subjected to local damage due to missile impact are:

- 44-inch thick roof
- 42-inch thick (minimum) front wall
- 36-inch thick end shield wall
- 36-inch thick rear shield wall
- 30.5-inch thick shielding door

The minimum thickness of concrete target components listed above is 30.5 inches. So, the required perforation thickness and require scabbing thickness is compared against 30.5 inches to ensure the adequacy of design.

3.9.4.10.6.1.1 Local Impact Effects of Utility Wooden Pole Missile

Per section 6.4.1.2.5 of [3.9.4-13], utility wooden pole missiles do not have sufficient strength to penetrate a concrete target and that the scabbing thickness required for wood missiles is substantially less than that required for a steel missile with the same mass and velocity. Practically, wooden pole missiles do not appear to be capable of causing local damage to the 12-inch or thicker walls (also see Section 2.1.1 of [3.9.4-18]). Since none of the concrete targets are less than 12 inches thick, the postulated wood missiles do not cause any local damage to the EOS-HSM concrete component.

3.9.4.10.6.1.2 Local Impact Effects of Armor Piercing Artillery Shell Missile

The penetration depth for this missile is calculated using the NDRC Formula as given in Section 3.9.4.10.6.1 (a) and the parameters used in the formula are as listed below:

d = 8.0 in.	effective diameter of missile
W = 276 lb	weight of missile
v_o = 185 fps	striking velocity of missile
f'_c = 5000 psi	concrete compressive strength
K = 180/√5000 = 2.55	concrete penetrability factor
N = 0.84	projectile shape factor (blunt nosed)
Penetration depth, x = 4.6 in.	for x/d (= 0.58) ≤ 2.0
Perforation thickness, e = 12.9 in.	for x/d (= 0.58) ≤ 1.35

Required perforation thickness = 1.2*12.9 = 15.5 in. < 30.5 in.

Scabbing thickness, s = 23.1 in. for x/d (= 0.58) ≤ 0.65

Required scabbing thickness = 1.2*23.1 = 27.7 in. < 30.5 in.

Therefore, penetration, perforation and scabbing of the concrete components of EOS-HSM do not occur due to this missile impact.

3.9.4.10.6.1.3 Local Impact Effects of 12-Inch Diameter Schedule 40 Steel Pipe Missile

The penetration depth for this missile is calculated using the NDRC Formula as given in Section 3.9.4.10.6.1 (A) and the parameters used in the formula are as listed below:

ϕ = 12.75 in.	outer diameter of 12” dia. schedule 40 steel pipe.
A_c = 15.74 in^2	missile impact area (cross sectional area of steel)

$d = (4*15.74/\pi)^{1/2} = 4.5$ in. effective diameter of missile

W = 750 lb weight of missile

v_o = 154 fps striking velocity of missile

f'_c = 5000 psi concrete compressive strength

K = 180/√5000 = 2.55 concrete penetrability factor

N = 0.72 projectile shape factor (flat nosed)

Penetration depth, x = 7.6 in. for x/d (= 1.69) ≤ 2.0

Perforation thickness, e = 15.4 in. for 1.35 ≤ x/d (= 1.69) ≤ 13.5

Required perforation thickness = 1.2*15.4 = 18.5 in. < 30.5 in. OK

Scabbing thickness, s = 19.9 in. for 0.65 ≤ x/d (= 1.69) ≤ 11.75

Required scabbing thickness = 1 .2*19.9 = 23.9 in. < 30.5 in. OK

Therefore, penetration, perforation and scabbing of the concrete components of EOS-HSM do not occur due to this missile impact.

3.9.4.10.6.2 Global Structural Response

When a missile strikes a structure, large forces develop at the missile-structure interface, which decelerate the missile and accelerate the structure. The response of the structure depends on the dynamic properties of the structure and the time dependent nature of the applied loading (interface force-time function). The force-time function is, in turn, dependent on the type of impact (elastic or plastic) and the nature and extent of local damage.

In an elastic impact, the missile and the structure deform elastically, remain in contact for a short period of time (duration of impact), and subsequently disengage due to the action of elastic interface restoring forces.

In a plastic impact, the missile or the structure (or both) may sustain permanent deformation or damage (local damage). Elastic restoring forces are small, and the missile and the structure tend to remain in contact after impact. Plastic impact is much more common than elastic impact, which is rarely encountered. Test data have indicated that the impact from all postulated tornado-generated missiles can be characterized as a plastic impact.

If the interface forcing function can be defined or conservatively idealized, the structure can be modeled mathematically, and conventional analytical or numerical techniques can be used to predict structural response. If the interface forcing function cannot be defined, the same mathematical model of the structure can be used to determine structural response by application of conservation of momentum and energy balance techniques with due consideration for type of impact (elastic or plastic).

In either case, in lieu of a more rigorous analysis, a conservative estimate of structural response can be obtained by first determining the response of the impacted structural element, and then applying its reaction forces to the supporting structure. The predicted structural response enables assessment of structural design adequacy in terms of strain energy capacity, deformation limits, stability and structural integrity.

The overall structural response of each component as a whole (global response) is determined by single degree of freedom analysis using response charts solution method of [3.9.4-18].

The following enveloping missiles are considered for global structural response:

- Utility wooden pole
- Armor piercing artillery shell
- 12-inch diameter schedule 40 steel pipe
- Automobile missile

The peak interface force and impact duration for each missile are calculated as follows:

A. Utility Wooden Pole Missile

For wooden missile, the interface forcing function is a rectangular pulse having a force magnitude of F and duration t_i, per Section 2.3.1 of [3.9.4-18]

$F = PA$

$t_i = M_m \nu_c / F$

Where,

F = interface force (lb)

P = interface pressure (psi) = 2500 psi for wood missiles [3.9.4-18]

A = cross sectional area of the missile (in^2) = π * 13.52/4 = 143.1 in^2

t_i = impact duration (sec)

W_m = weight of missile (lb) = 1124 lb

M_m = missile mass (lb-sec^2/ft) = W_m/g = 1124 lb /32.2 ft/sec^2 = 34.9 lb-sec^2/ft

ν_c = change in velocity during impact (conservatively = ν_s) (fps) = 180 fps

Therefore,

F = 358 kip and t_i = 0.018 sec

B. Armor Piercing Artillery Shell

For solid steel missile, the concrete is a soft target per section 6.4.2 of [3.9.4-13] with a penetration depth of 4.6 in. The interface forcing function is a rectangular pulse per Section 6.4.2.1.1 of [3.9.4-13].

$F = W_m V_0^2/2gX$

$t_i = 2X/V_0$

Where,

F = interface force (lb)

t_i = impact duration (sec)

W_m = missile weight (lb) = 276 lb

V_0 = initial velocity of the missile (fps) = 185 fps

X = penetration depth = 4.6 in.

Therefore,

F = 383 kip and t_i = 0.00414 sec

C. 12-Inch Diameter Schedule 40 Steel Pipe

For steel pipe missile, the interface forcing function is a triangular pulse per Section 2.3.2 of [3.9.4-18].

$t_i = 400M_m /PA$

$F = (2M_m\nu_s)/t_i$

Where,

F = peak interface force (lb)

P = collapse stress of pipe (psi) = 60000 psi

A = cross sectional metal area of the missile (in^2) = 15.74 in^2

t_i = impact duration (sec)

W_m = weight of missile (lb) = 750 lb

M_m = missile mass (lb-sec^2/ft) = W_m/g = 750 lb /32.2 ft/sec^2 = 23.29 lb-sec^2/ft

ν_s = striking velocity of missile = 154 fps

Therefore,

F = 718 kip and t_i = 0.01 sec

D. Automobile Missile

For automobile missile, the interface forcing function per 2.3.3 of [3.9.4-18] is as follows:

$F_t = 0.625\ v_c\ W \sin(20t)$ $0 < t \leq 0.0785$ sec

$F_t = 0$ $t > 0.0785$ sec

Where,

F_t = force as a function of time (lb)

W = weight of automobile (lb) = 4000 lb

v_c = change in velocity during impact (conservatively = v_s) (fps) = 195 fps

Therefore,

F = 488 kip and t_i = 0.0785 sec

The end wall, rear wall, base front wall, roof and door of EOS-HSM are evaluated for global response, since these components may interface with missile loading. The end/rear walls and door are idealized as a simply supported plate while the base front wall and roof are idealized as simply supported beam for structural response. The yield resistance and fundamental period of vibration of concrete components is then determined based on the assumed idealized boundary condition using the equations given in Section 4.4 of [3.9.4-18]. The calculated value of yield resistance, R_y, and fundamental period of vibration, T_n, for different concrete components are tabulated below.

Component	R_y (kip)	T_n (sec)
End Wall	446.1	0.0180
Rear Wall	919.9	0.0065
Base Front Wall	1182.5	0.0045
Roof	402.0	0.0301
Door	1211.0	0.002124

In the response chart solution method, the structural response is determined by entering the chart with calculated values of C_T and C_R to determine the ductility ratio, μ, which is compared against the allowable ductility ratio as given in Appendix F of ACI 349-06 [3.9.4-12]. The dimensionless ratios, C_T and C_R, are defined as follows:

$$C_R = \frac{R_y}{F} \qquad C_T = \frac{t_i}{T_n}$$

The maximum value of ductility ratio of all five components is found to be less than 10. The allowable ductility ratio per ACI 349-06 [3.9.4-12] is 10. Hence, the global response of EOS-HSM is within deformation limit meeting the ductility requirement.

Each component is also evaluated for punching shear capacity with interfacing utility wooden pole missile and automobile missile. All the components have punching shear capacity greater than the peak missile interface force.

3.9.4.11 Conclusions

The load categories associated with normal operating conditions, off-normal conditions and postulated accident conditions are described and analyzed in previous sections. The load combination results for EOS-HSM components important-to-safety are also presented. Comparison of the results with the corresponding design capacity shows that the design strength of the EOS-HSM is greater than the strength required for the most critical load combination.

3.9.4.12 References

3.9.4-1 Code of Federal Regulation Title 10, Part 72 (10CFR Part 72), "Licensing Requirements for the Independent Storage of Spent Nuclear Fuel, High-Level Radioactive Waste, and Reactor-Related Greater than Class C Waste."

3.9.4-2 U.S. Nuclear Regulatory Commission, Regulatory Guide 1.60, "Design Response Spectra for Seismic Design of Nuclear Power Plants," Revision 1, 1973.

3.9.4-3 U.S. Nuclear Regulatory Commission, Regulatory Guide 1.61, "Damping Values for Seismic Design of Nuclear Power Plants," Revision 1, March 2007.

3.9.4-4 U.S. Nuclear Regulatory Commission, Regulatory Guide 1.76, "Design Basis Tornado for Nuclear Power Plants," Revision 0, April 1974.

3.9.4-5 U.S. Nuclear Regulatory Commission, Regulatory Guide 1.92, "Combining Modal Responses and Spatial Components in Seismic Response Analysis," Revision 3, October 2012.

3.9.4-6 U.S. Nuclear Regulatory Commission, Regulatory Guide 1.122, "Development of Floor Design Response Spectra for Seismic Design of Floor-Supported Equipment or Components," Revision 1, 1978.

3.9.4-7 NUREG-0800, Standard Review Plan, Section 3.5.1.4, "Missiles Generated by Natural Phenomena," Revision 2, July 1981.

3.9.4-8 NUREG-0800, Standard Review Plan, Section 3.3.1, "Wind Loading," Section 3.3.2 "Tornado Loads," and Section 3.5.1.4 "Missiles Generated by Tornado and Extreme Winds," Revision 3, March 2007.

3.9.4-9 NUREG-1536, "Standard Review Plan for Spent Fuel Dry Storage Systems at a General License Facility," Revision 1, U.S. Nuclear Regulatory Commission, July 2010.

3.9.4-10 ANSI/ANS 57.9-1984, "Design Criteria for an Independent Spent Fuel Storage Installation (Dry Storage Type)," American National Standards Institute, American Nuclear Society.

3.9.4-11 ACI-318-08, "Building Code Requirement for Structural Concrete," American Concrete Institute.

3.9.4-12 ACI 349-06, "Code Requirements for Nuclear Safety Related Concrete Structures," American Concrete Institute.

3.9.4-13 American Society of Civil Engineers, "Structural Analysis and Design of Nuclear Plant Facilities," ASCE Publication No. 58.

3.9.4-14 American Institute of Steel Construction, AISC Manual of Steel Construction, 13th Edition.

3.9.4-15 American Society of Civil Engineers, "Minimum Design Loads for Buildings and Other Structures," ASCE 7-10 (formerly ANSI A58.1).

3.9.4-16 AREVA Inc., "Updated Final Safety Analysis Report for the Standardized NUHOMS® Horizontal Modular Storage System for Irradiated Nuclear Fuel," Revision 14, USNRC Docket Number 72-1004, September 2014.

3.9.4-17 Bechtel Power Corporation, "Design of Structures for Missile Impact," Topical Report BCTOP-9A, Revision 2, San Francisco, California.

3.9.4-18 Bechtel Corporation, "Design Guide Number C-2.45 for Design of Structures for Tornado Missile Impact," Rev. 0, April 1982.

3.9.4-19 "ANSYS Computer Code and User's Manual", Release 14.0.3.

3.9.4-20 Binder, Raymond C., "Fluid Mechanics," 3rd Edition, Prentice-Hall, Inc, 1973.

3.9.4-21 AREVA Inc., "Updated Final Safety Analysis Report For The Standardized Advanced NUHOMS® Horizontal Modular Storage System For Irradiated Nuclear Fuel," Revision 6, US NRC Docket Number 72-1029, August 2014.

3.9.4-22 U.S. Nuclear Regulatory Commission, Regulatory Guide 1.76, "Design Basis Tornado for Nuclear Power Plants," Revision 1, March 2007.

Table 3.9.4-1
Design Pressures for Tornado Wind Flowing from Front Wall to Rear Wall and Vice Versa

Component	Velocity Pressure, q_v (psf)	External Pressure Coefficient, C_p	Internal Pressure Coefficient, (GC_{pi})	Max. Design Pressure, $q_v*(G*C_p-GC_{pi})$ (psf)
Windward(Front/Rear Wall)	254	0.80	±0.18	218
Leeward(Rear/Front Wall)		-0.30(1)		-110
Side(Right Side Wall)		-0.70		-197
Side(Left Side Wall)		-0.70		-197
Roof		-1.30		-326

Notes:

1. The C_p value is taken for L/B = 268”/116” ≈ 2.0.
2. The gust effect factor, G=0.85 considering the EOS-HSM as rigid.

Table 3.9.4-2
Design Pressures for Tornado Wind Flowing from Right Side to Left Side Wall and Vice Versa

Component	Velocity Pressure, q_v (psf)	External Pressure Coefficient, C_p	Internal Pressure Coefficient, (GC_{pi})	Max. Design Pressure, $q_v*(G*C_p-GC_{pi})$ (psf)
Side(Front Wall)	254	-0.70	±0.18	-197
Side(Rear Wall)		-0.70		-197
Windward(Right/Left Side Wall)		0.80		218
Leeward(Left/Right Side Wall)		-0.50(1)		-154
Roof		-1.30		-326

Notes:

1. The C_p value is taken for L/B = 116”/268” ≈ 0.4
2. The gust effect factor, G=0.85 considering the EOS-HSM as rigid.

Table 3.9.4-3
Spectral Acceleration Applicable to Different Components of EOS-HSM for Seismic Analysis

Direction	Frequency (Hz)	Spectral Acceleration Corresponding to ZPA = 0.5g horizontal & 0.333 g vertical[1]		
		at 3% Damping (for DSC)	at 4% Damping (for DSC support structure)	at 7% Damping (for concrete components)
X (Transverse)	18.7	1.229g	1.156g	0.936g
Y (Vertical)	60.3	0.333g	0.333g	0.333g
Z (Longitudinal)	32.7	0.694g	0.677g	0.628g

(1) Seismic loading conservatively exceeds the design basis ZPA values of 0.45g horizontal and 0.30g vertical.

Table 3.9.4-4
Load Cases for EOS-HSM Concrete Components Evaluation

Design Load Type	Load Notation	Design Parameters	Applicable Codes / References
Normal			
Dead	DL	Includes self-weight with 160 pcf density for concrete and 0.28 pci for steel support structure.	ANSI/ANS 57.9-1984 [3.9.4-10]
Live	LL	Design live load of 200 psf on roof which includes snow and ice load and DSC weight of 135 kip applied on DSC support rails.	ANSI/ANS 57.9-1984 [3.9.4-10] & ASCE 7-10 [3.9.4-15]
Normal Handling	R_O	The concrete module is evaluated for 140 kip DSC insertion load as a normal handling load. The DSC weight is also applied at both rail support locations (4 points).	
Normal Thermal	T_O	DSC with spent fuel rejecting up to 50.0 kW of decay heat. Extreme ambient air temp. -20°F and 100°F. Reference temperature = 70°F.	
Off-Normal/Accidental			
Off-Normal Handling	R_a	For the steel support structure the magnitude of this load is 135 kip both for DSC insertion and retrieval, applied to one rail. The DSC weight is also applied at one rail support location (two points).	
Accidental Thermal	T_a	Enveloped of Off-Normal and Accidental Thermal (vent blocked) condition. Accidental thermal condition is same as off-normal condition with ambient temperature range of -40°F to 117°F. Reference temperature = 70°F	
Earthquake	E	Zero period acceleration of 0.5g in horizontal and 0.333g in vertical direction with enhancement in frequency above 9 Hz and 7% damping. (1)	NRC Reg. Guide 1.60 [3.9.4-2] & Reg. Guide 1.61 [3.9.4-3]
Flood	FL	Maximum flood height of 50 ft and max. velocity of water 15 ft/sec	10 CFR Part 72 [3.9.4-1]
Wind/Tornado Wind	W/W_t	Maximum wind speed of 360 mph, and a pressure drop of 3 psi	ASCE 7-10 [3.9.4-15] & NRC Reg Guide 1.76 [3.9.4-4]
Tornado Generated Missile	W_m	4 types of tornado-generated missiles	NUREG-0800 Section 3.5.1.4 [3.9.4-7]

(1) Seismic loading conservatively exceeds the design basis ZPA values of 0.45g horizontal and 0.30g vertical.

Table 3.9.4-5
Load Combination for EOS-HSM Concrete Components Evaluation

Combination Number	Load Combination	Event
C1	1.4 DL + 1.7 (LL + R_o)	Normal
C2	1.05 DL + 1.275 (LL + T_o + W)	Off-Normal – Wind
C3	1.05 DL + 1.275 (LL + T_o + R_a)	Off-Normal – Handling
C4	DL + LL + T_o + E	Accident – Earthquake
C5	DL + LL + T_o + W_t	Accident – Tornado
C6	DL + LL + T_o + FL	Accident – Flood
C7	DL + LL + Ta	Accident – Thermal

Note: See Table 3.9.4-4 for notation.

Table 3.9.4-6
Strength Reduction Factors for Concrete

Type of Stress	Strength Reduction Factor, ϕ
Tension - Controlled	0.90
Compression - Controlled	0.65
Shear	0.75
Torsion	0.75
Bearing	0.65

Note: The strength reduction factors are taken from ACI 349-06, Section 9.3 [3.9.4-12].

Table 3.9.4-7
Demand of EOS-HSM Concrete Components for Shear Forces and Moments

Component	Load Combination	M_1 (in-kip/ft)	M_2 (in-kip/ft)	V_{o1} (kip/ft)	V_{o2} (kip/ft)	V_i (kip/ft)
1. Rear Wall Bottom (32”)	C1 through C6	338.7	708.7	6.3	9.8	51.6
	C7	232.8	270.8	1.9	2.7	25.3
2. Rear Wall Top (12”)	C1 through C6	36.9	106.6	5.1	6.4	13.7
	C7	24.5	69.3	4.2	2.9	7.6
3. Front Wall Bottom (54”)	C1 through C6	1024.0	1877.2	14.2	13.0	57.6
	C7	1049.1	1735.2	3.1	3.1	25.2
4. Front Wall Top (42”)	C1 through C6	949.7	1768.7	28.5	25.6	90.4
	C7	1353.1	2485.3	26.1	24.4	48.3
5. Side Wall Bottom (24”)	C1 through C6	269.3	182.9	15.4	14.8	23.5
	C7	143.4	396.3	14.3	18.6	11.1
6. Side Wall Bottom (14”)	C1 through C6	91.4	38.0	11.4	6.1	14.4
	C7	64.0	117.2	12.1	12.7	11.1
7. Side Wall Top (12”)	C1 through C6	285.3	195.0	12.3	11.9	38.5
	C7	341.2	151.8	10.6	10.6	46.5
8. Roof (44”)	C1 through C6	622.2	1831.5	46.1	49.5	21.5
	C7	283.6	1004.2	11.6	24.3	22.5

Table 3.9.4-8
Demand of EOS-HSM Concrete Components for Axial Forces and Moments

Component	Load Combination	T_1 (kip/ft)	T_2 (kip/ft)	C_1 (kip/ft)	C_2 (kip/ft)	M_{1P} (in-kip/ft)	M_{2P} (in-kip/ft)
1. Rear Wall Bottom (32”)	C1 through C6	33.8	32.1	46.4	104.4	299.6	428.3
	C7	13.4	5.5	40.5	44.6	66.4	124.1
2. Rear Wall Top (12”)	C1 through C6	9.5	23.6	7.5	29.6	36.9	43.4
	C7	7.1	40.0	15.1	15.8	20.1	45.8
3. Front Wall Bottom (54”)	C1 through C6	72.2	65.6	51.3	122.3	1019.5	773.8
	C7	19.8	0.0	32.0	59.8	485.3	0.0
4. Front Wall Top (42”)	C1 through C6	97.7	77.5	86.6	256.2	737.5	1137.7
	C7	22.1	32.8	38.7	98.9	1352.7	1796.9
5. Side Wall Bottom (24”)	C1 through C6	28.0	37.6	48.2	70.2	267.5	158.6
	C7	22.5	58.7	28.0	38.8	97.1	324.9
6. Side Wall Bottom (14”)	C1 through C6	19.4	16.5	47.6	15.9	75.9	37.9
	C7	31.5	62.9	21.9	6.1	64.0	117.2
7. Side Wall Top (12”)	C1 through C6	27.5	49.7	157.1	103.7	44.4	49.0
	C7	56.9	11.7	138.0	108.7	64.5	132.3
8. Roof (44”)	C1 through C6	24.4	67.5	35.4	107.1	621.8	1817.3
	C7	11.5	59.9	4.8	90.8	239.4	751.2

Table 3.9.4-9
Demand of EOS-HSMS Concrete Components for Shear Forces and Moments

Component	Load Combination	M_1 (in-kip/ft)	M_2 (in-kip/ft)	V_{o1} (kip/ft)	V_{o2} (kip/ft)	V_i (kip/ft)
1. Rear Wall Bottom (32”)	C1 through C6	335.6	694.6	6.9	11.3	55.5
	C7	215.2	297.1	2.2	2.5	24.5
2. Rear Wall Top (12”)	C1 through C6	69.4	110.3	4.9	7.7	52.9
	C7	25.1	66.2	3.2	3.0	8.5
3. Front Wall Bottom (54”)	C1 through C6	970.2	1882.1	13.4	13.0	60.8
	C7	1028.4	1436.7	3.6	3.1	26.2
4. Front Wall Top (42”)	C1 through C6	1077.5	1501.8	28.7	28.3	130.5
	C7	1500.8	2424.0	24.8	21.4	46.8
5. Side Wall Bottom (24”)	C1 through C6	193.1	161.2	13.3	12.6	20.9
	C7	140.6	409.0	14.6	17.4	13.1
6. Side Wall Bottom (14”)	C1 through C6	67.4	38.9	10.9	6.6	15.4
	C7	58.5	115.7	12.0	12.0	9.8
7. Side Wall Top (12”)	C1 through C6	265.9	224.6	12.1	12.1	59.3
	C7	307.9	138.6	10.6	10.6	37.7
8. Roof (44”)	C1 through C6	623.2	1839.1	39.3	49.8	22.3
	C7	291.1	979.2	10.2	21.8	20.8

Table 3.9.4-10
Demand of EOS-HSMS Concrete Components for Axial Forces and Moments

Component	Load Combination	T_1 (kip/ft)	T_2 (kip/ft)	C_1 (kip/ft)	C_2 (kip/ft)	M_{1P} (in-kip/ft)	M_{2P} (in-kip/ft)
1. Rear Wall Bottom (32”)	C1 through C6	25.0	42.4	49.3	108.5	248.3	344.0
	C7	14.6	10.9	39.7	47.3	58.8	295.8
2. Rear Wall Top (12”)	C1 through C6	51.4	43.7	306.1	132.2	44.1	29.1
	C7	7.5	34.8	21.9	22.4	21.2	42.4
3. Front Wall Bottom (54”)	C1 through C6	54.1	88.6	75.0	117.7	800.5	412.6
	C7	20.5	0.0	35.3	62.5	486.1	0.0
4. Front Wall Top (42”)	C1 through C6	111.6	103.8	426.5	336.5	352.2	907.9
	C7	45.6	80.0	65.8	163.9	1500.8	992.9
5. Side Wall Bottom (24”)	C1 through C6	34.7	28.2	49.3	60.0	181.8	159.6
	C7	21.0	55.2	26.4	33.8	98.8	342.5
6. Side Wall Bottom (14”)	C1 through C6	20.6	15.0	45.9	16.8	64.3	38.9
	C7	29.8	57.3	21.0	10.2	57.2	115.7
7. Side Wall Top (12”)	C1 through C6	50.8	62.0	257.1	233.8	40.9	63.2
	C7	51.8	58.5	121.8	240.2	63.3	62.7
8. Roof (44”)	C1 through C6	24.9	76.4	38.8	114.5	623.0	1824.9
	C7	10.4	46.9	4.9	94.0	246.1	746.4

Table 3.9.4-11
Ultimate Shear/Moment Capacities of Concrete Components

Component	Thermal Condition	V_{ui} kips/ft	V_{uo1} kips/ft	V_{uo2} kips/ft	M_{u1} kip-in/ft	M_{u2} kip-in/ft
1. Rear Wall Bottom (32")	Normal	90.4	38.3	38.3	886.8	886.8
	Accident	85.6	36.3	36.3	837.1	837.1
2. Rear Wall Top (12")	Normal	65.0	12.8	12.8	290.4	290.4
	Accident	61.4	12.2	12.2	273.8	273.8
3. Front Wall Bottom (54")	Normal	196.0	64.3	64.3	3,791.7	3,791.7
	Accident	185.4	61.0	61.0	3,578.1	3,578.1
4. Front Wall Top (42")	Normal	180.7	49.0	49.0	2,875.6	2,875.6
	Accident	170.9	46.5	46.5	2,712.9	2,712.9
5. Side Wall Bottom (24")	Normal	102.1	27.8	27.8	919.3	919.3
	Accident	96.6	26.4	26.4	867.3	867.3
6. Side Wall Bottom (14")	Normal	89.4	15.1	15.1	489.8	489.8
	Accident	84.5	14.3	14.3	461.7	461.7
7. Side Wall Top (12")	Normal	86.8	12.6	12.6	404.0	404.0
	Accident	82.1	11.9	11.9	380.6	380.6
8. Roof (44")	Normal	151.4	51.5	51.5	2,283.1	2,283.1
	Accident	143.3	48.9	48.9	2,154.6	2,154.6

Notes:

V_{ui} = Minimum of ultimate in plane shear capacities in planes 1 and 2.
V_{uo1} = Minimum ultimate out of plane shear capacity in plane 1.
V_{uo2} = Minimum ultimate out of plane shear capacity in plane 2.
M_{u1} = Minimum ultimate moment capacity in plane 1.
M_{u2} = Minimum ultimate moment capacity in plane 2.
Planes 1 and 2 are defined in Figure 3.9.4-5.

Table 3.9.4-12
Ultimate Axial/Moment Capacities of Concrete Components

Component	Thermal Condition	P_{tu} kips/ft	P_{cu} kips/ft	P_{ub1} kips/ft	P_{ub2} kips/ft	M_{ub1} kip-in/ft	M_{ub2} kip-in/ft
1. Rear Wall Bottom (32")	Normal	59.6	880.4	490.2	490.2	4,802.8	4,802.8
	Accident	56.3	793.9	465.0	465.0	4,367.5	4,367.5
2. Rear Wall Top (12")	Normal	59.6	350.0	163.0	163.0	747.1	747.1
	Accident	56.3	316.5	154.6	154.6	687.3	687.3
3. Front Wall Bottom (54")	Normal	152.7	1,513.4	822.0	822.0	14,501.4	14,501.4
	Accident	144.2	1,365.9	779.7	779.7	13,222.4	13,222.4
4. Front Wall Top (42")	Normal	152.7	1,195.1	625.7	625.7	9,097.3	9,097.3
	Accident	144.2	1,079.5	593.5	593.5	8,318.6	8,318.6
5. Side Wall Bottom (24")	Normal	85.9	682.2	355.5	355.5	2,951.3	2,951.3
	Accident	81.1	616.2	337.2	337.2	2,699.1	2,699.1
6. Side Wall Bottom (14")	Normal	85.9	417.0	191.9	191.9	1,081.2	1,081.2
	Accident	81.1	377.5	182.1	182.1	995.7	995.7
7. Side Wall Top (12")	Normal	85.9	364.0	159.1	159.1	806.6	806.6
	Accident	81.1	329.8	151.0	151.0	744.4	744.4
8. Roof (44")	Normal	114.5	1,227.8	659.5	659.5	9,425.2	9,425.2
	Accident	108.1	1,108.0	625.5	625.5	8,597.8	8,597.8

Notes:

P_{tu} = Minimum of ultimate tensile capacities in planes 1 and 2.
P_{cu} = Minimum of ultimate compressive capacities in plane 1 and 2.
P_{ub1} = Minimum of ultimate balanced section compressive capacity in plane 1.
P_{ub2} = Minimum of ultimate balanced section compressive capacity in plane 2.
M_{ub1} = Minimum of ultimate balanced section moment capacity in plane 1.
M_{ub2} = Minimum of ultimate balanced section moment capacity in plane 2.
Planes 1 and 2 are defined in Figure 3.9.4-5.

Table 3.9.4-13
Comparison of Highest Combined Shear Forces/Moments with the Capacities of EOS-HSM
3 Pages

Component	Load Combination	Quantity	V_I Kips/ft	V_{o1} kips/ft	V_{o2} kips/ft	M_1 kip-in/ft	M_2 kip-in/ft
1. Rear Wall Bottom (32")	C1 through C6	Computed	51.62	6.26	9.79	338.75	708.70
		Capacity	90.43	38.26	38.26	886.79	886.79
		Ratio	0.57	0.16	0.26	0.38	0.80
	C7	Computed	25.29	1.86	2.71	232.79	270.83
		Capacity	85.58	36.30	36.30	837.08	837.08
		Ratio	0.30	0.05	0.07	0.28	0.32
2. Rear Wall Top (12")	C1 through C6	Computed	13.70	5.12	6.40	36.93	106.65
		Capacity	64.97	12.81	12.81	290.38	290.38
		Ratio	0.21	0.40	0.50	0.13	0.37
	C7	Computed	7.64	4.22	2.95	24.52	69.33
		Capacity	61.43	12.15	12.15	273.80	273.80
		Ratio	0.12	0.35	0.24	0.09	0.25
3. Front Wall Bottom (54")	C1 through C6	Computed	57.56	14.24	13.02	1023.97	1877.23
		Capacity	195.97	64.28	64.28	3791.72	3791.72
		Ratio	0.29	0.22	0.20	0.27	0.50
	C7	Computed	25.23	3.12	3.11	1049.12	1735.23
		Capacity	185.37	60.98	60.98	3578.11	3578.11
		Ratio	0.14	0.05	0.05	0.29	0.48

Table 3.9.4-13
Comparison of Highest Combined Shear Forces/Moments with the Capacities of EOS-HSM
3 Pages

Component	Load Combination	Quantity	V_I Kips/ft	V_{o1} kips/ft	V_{o2} kips/ft	M_1 kip-in/ft	M_2 kip-in/ft
4. Front Wall Top (42")	C1 through C6	Computed	90.42	28.50	25.62	949.69	1768.70
		Capacity	180.69	49.00	49.00	2875.63	2875.63
		Ratio	0.50	0.58	0.52	0.33	0.62
	C7	Computed	48.32	26.12	24.35	1353.14	2485.27
		Capacity	170.88	46.49	46.49	2712.91	2712.91
		Ratio	0.28	0.56	0.52	0.50	0.92
5. Side Wall Bottom (24")	C1 through C6	Computed	23.50	15.39	14.78	269.28	182.86
		Capacity	102.12	27.84	27.84	919.26	919.26
		Ratio	0.23	0.55	0.53	0.29	0.20
	C7	Computed	11.06	14.31	18.56	143.44	396.28
		Capacity	96.57	26.41	26.41	867.25	867.25
		Ratio	0.11	0.54	0.70	0.17	0.46
6. Side Wall Bottom (14")	C1 through C6	Computed	14.39	11.42	6.10	91.36	38.03
		Capacity	89.39	15.11	15.11	489.85	489.85
		Ratio	0.16	0.76	0.40	0.19	0.08
	C7	Computed	11.13	12.14	12.65	63.98	117.21
		Capacity	84.50	14.34	14.34	461.69	461.69
		Ratio	0.13	0.85	0.88	0.14	0.25

Table 3.9.4-13
Comparison of Highest Combined Shear Forces/Moments with the Capacities of EOS-HSM
3 Pages

Component	Load Combination	Quantity	V_I Kips/ft	V_{o1} kips/ft	V_{o2} kips/ft	M_1 kip-in/ft	M_2 kip-in/ft
7. Side Wall Top (12")	C1 through C6	Computed	38.48	12.32	11.88	285.32	195.00
		Capacity	86.84	12.57	12.57	403.96	403.96
		Ratio	0.44	0.98	0.95	0.71	0.48
	C7	Computed	46.54	10.56	10.64	341.15	151.85
		Capacity	82.08	11.92	11.92	380.58	380.58
		Ratio	0.57	0.89	0.89	0.90	0.40
8. Roof (44")	C1 through C6	Computed	21.46	46.12	49.54	622.18	1831.53
		Capacity	151.43	51.55	51.55	2283.14	2283.14
		Ratio	0.14	0.89	0.96	0.27	0.80
	C7	Computed	22.51	11.56	24.29	283.58	1004.18
		Capacity	143.25	48.90	48.90	2154.63	2154.63
		Ratio	0.16	0.24	0.50	0.13	0.47

Notes:

Load Combinations C1 through C6 include normal thermal condition and C7 includes accidental thermal condition.

Table 3.9.4-14
Comparison of Highest Combined Axial Forces/Moments with the Capacities of EOS-HSM
3 Pages

Component	Load Combination	Quantity	P (Comp) kips/ft	P_1 (Tens) kips/ft	P_2 (Tens.) kips/ft	M_{1p} (1) kip-in/ft	M_{2p} (1) kip-in/ft
1. Rear Wall Bottom (32")	C1 through C6	Computed	104.39	33.78	32.11	299.64	428.28
		Capacity	880.39	59.64	59.64	427.42	738.10
		Ratio	0.12	0.57	0.54	0.70	0.58
	C7	Computed	44.56	13.37	5.46	66.43	124.05
		Capacity	793.88	56.33	56.33	826.20	806.31
		Ratio	0.06	0.24	0.10	0.08	0.15
2. Rear Wall Top (12")	C1 through C6	Computed	29.63	9.50	23.56	36.93	43.42
		Capacity	349.99	59.64	59.64	279.91	238.59
		Ratio	0.08	0.16	0.40	0.13	0.18
	C7	Computed	15.84	7.09	40.00	20.08	45.85
		Capacity	316.52	56.33	56.33	249.52	79.84
		Ratio	0.05	0.13	0.71	0.08	0.57
3. Front Wall Bottom (54")	C1 through C6	Computed	122.27	72.22	65.59	1019.49	773.80
		Capacity	1513.35	152.68	152.68	1998.10	3368.23
		Ratio	0.08	0.47	0.43	0.51	0.23
	C7	Computed	59.82	19.82	0.00	485.33	0.00
		Capacity	1365.94	144.20	144.20	3244.10	3578.11
		Ratio	0.04	0.14	0.00	0.15	0.00

Table 3.9.4-14
Comparison of Highest Combined Axial Forces/Moments with the Capacities of EOS-HSM
3 Pages

Component	Load Combination	Quantity	P (Comp) kips/ft	P_1 (Tens) kips/ft	P_2 (Tens.) kips/ft	M_{1p} (1) kip-in/ft	M_{2p} (1) kip-in/ft
4. Front Wall Top (42")	C1 through C6	Computed	256.17	97.70	77.54	737.46	1137.66
		Capacity	1195.11	152.68	152.68	2524.84	1880.68
		Ratio	0.21	0.64	0.51	0.29	0.60
	C7	Computed	98.93	22.08	32.83	1352.68	1796.91
		Capacity	1079.52	144.20	144.20	2297.59	2299.51
		Ratio	0.09	0.15	0.23	0.59	0.78
5. Side Wall Bottom (24")	C1 through C6	Computed	70.20	27.97	37.58	267.46	158.64
		Capacity	682.20	85.88	85.88	664.87	738.53
		Ratio	0.10	0.33	0.44	0.40	0.21
	C7	Computed	38.81	22.46	58.73	97.14	324.92
		Capacity	616.18	81.11	81.11	627.12	331.04
		Ratio	0.06	0.28	0.72	0.15	0.98
6. Side Wall Bottom (14")	C1 through C6	Computed	47.63	19.43	16.50	75.91	37.93
		Capacity	417.00	85.88	85.88	450.17	484.24
		Ratio	0.11	0.23	0.19	0.17	0.08
	C7	Computed	21.85	31.53	62.90	63.98	117.21
		Capacity	377.50	81.11	81.11	337.69	236.42
		Ratio	0.06	0.39	0.78	0.19	0.50

Table 3.9.4-14
Comparison of Highest Combined Axial Forces/Moments with the Capacities of EOS-HSM
3 Pages

Component	Load Combination	Quantity	P (Comp) kips/ft	P_1 (Tens) kips/ft	P_2 (Tens.) kips/ft	M_{1p} (1) kip-in/ft	M_{2p} (1) kip-in/ft
7. Side Wall Top (12")	C1 through C6	Computed	157.07	27.52	49.71	44.42	49.00
		Capacity	363.96	85.88	85.88	386.56	170.14
		Ratio	0.43	0.32	0.58	0.11	0.29
	C7	Computed	138.02	56.91	11.68	64.54	132.35
		Capacity	329.77	81.11	81.11	114.93	358.64
		Ratio	0.42	0.70	0.14	0.56	0.37
8. Roof (44")	C1 through C6	Computed	107.11	24.43	67.55	621.82	1817.34
		Capacity	1227.83	114.51	114.51	2237.29	2106.43
		Ratio	0.09	0.21	0.59	0.28	0.86
	C7	Computed	90.83	11.47	59.85	239.44	751.16
		Capacity	1107.99	108.15	108.15	2085.65	1488.26
		Ratio	0.08	0.11	0.55	0.11	0.50

Notes:

1. M_{1p} and M_{2p} are moments at the same location and for the same load combination as P_1 and P_2. M_{1p} and M_{2p} occur at the same location simultaneously with P_1 and P_2, i.e. $M_1 = [(P_{tu} - P_1)/P_{tu}]*M_{u1}$.
2. Load Combinations C1 to C6 include normal thermal, C7 include accident thermal.

Table 3.9.4-15
Load Cases for DSC Support Structure Evaluation

Load Type Nomenclature	Load Type Description
D	Dead load – self weight of rails
L	Live load – weight of the DSC
Ro	Normal handling load
To	Normal thermal load
Ra	Off-normal handling load
Ta	Envelope of off-normal and accident thermal loads
E	Earthquake load

Table 3.9.4-16
Load Combination for DSC Support Structure Evaluation

Load Combination ID	Load Combination	Event
N1	1.0 S > D + L + Ro	Normal
N2	1.0 S > D + L + Ro	Normal – Insertion/Extraction
N3	1.3 S > D + L + Ra + To	Off-normal – Handling
A5S	1.6 S > D + L + E + To	Accident – Earthquake
A5V	1.4 Sv > D + L + E + To	Accident – Earthquake
A8S	1.7 S > D + L + Ta	Accident – Thermal
A8V	1.4 Sv > D + L + Ta	Accident – Thermal

Table 3.9.4-17
Summary of Demand to Capacity Ratio (D/C Ratio) for the Whole Cross Section

Load Combination	Demand/Capacity Ratio	Maximum D/C Ratio and Controlling Action
N3 Strong	0.118	0.729 in Weak Axis Bending in load case A5 Seismic
N1 Weak	0.193	
A5S Weak	0.729	
A8S Weak	0.002	

Table 3.9.4-18
Summary of Demand to Capacity Ratio (D/C Ratio) for the Flange Elements

	Flange Demand/Capacity Type Ratio			Maximum D/C Ratio and Controlling Action
Load Combination	Axial Compression	Strong Bending	Weak Bending	
N1	0.314	0.02	0.228	0.388 Axial Compression in load case N3
N3	0.388	0.226	0.225	
A5S	0.265	0.022	0.229	
A8S	0.114	0.012	0.136	
N2	0.3	0.023	0.271	

Table 3.9.4-19
Summary of Demand to Capacity Ratio (D/C Ratio) for the Web Elements

Load Combination	Web Demand/Capacity Type Ratio			Maximum D/C Ratio and Controlling Action
	Axial Compression	Strong Bending	Weak Bending	
N1	0.747	0.08	0.012	0.761 in Axial Compression in load case A5 Seismic
N3	0.7	0.007	0.007	
A5S	0.761	0.076	0.014	
A8S	0.407	0.038	0.008	
N2	0.693	0.091	0.012	

Table 3.9.4-20
Summary of Demand to Capacity Ratio (D/C Ratio) for the Stiffener Elements

Load Combination	Stiffener Demand/Capacity Type Ratio			Maximum D/C Ratio and Controlling Action
	Axial Compression	Strong Bending	Weak Bending	
N1	0.162	0.023	0.707	0.805 in Weak Axis Bending in load case A5 Seismic
N3	0.059	0.372	0.372	
A5S	0.153	0.026	0.805	
A8S	0.096	0.014	0.434	
N2	0.156	0.02	0.529	

Table 3.9.4-21
Summary of Demand to Capacity Ratio (D/C Ratio) for the Accessories

Item	Demand/Capacity Ratio
Stop plate	0.784
DSC seismic impact	0.027
Extension baseplate	0.864
Lateral braces	0.636

Table 3.9.4-22
Summary of Demand to Capacity Ratio (D/C Ratio) for the Welds

Weld between	Demand/Capacity Ratio
Stop plate and rail	0.363
Extension baseplate and rail	0.141
Stiffener and lateral brace	0.291
Stiffener plate and rail	0.668

Table 3.9.4-23
Modal Frequencies and Mass Participation of EOS-HSMS3

Mode	Frequency (Hz)	Mass Participation					
		X-Direction		Y-Direction		Z-Direction	
		Mass (lb-s^2/in)	%	Mass (lb-s^2/in)	%	Mass (lb-s^2/in)	%
1	18.7	696	56%	-	-	-	-
2	31.7	-	-	-	-	-	-
3	32.7	-	-	-	-	711	57%
4	33.6	-	-	-	-	-	-
5	37.6	20	2%	-	-	-	-
6	49.8	291	23%	-	-	-	-
7	60.3	-	-	489	39%	-	-
8	67.3	-	-	-	-	323	26%
9	69.2	-	-	-	-	-	-
10	70.4	-	-	-	-	-	-

Table 3.9.4-24
Roof Heat Shield Modal Participating Mass Ratios

Frequency (Hz)	Participating Mass Ratio		
	X-Direction	Y-Direction	Z-Direction
5.86	0.026	0.000	0.000
7.40	0.000	0.000	0.573
11.29	0.000	0.000	0.000
12.71	0.003	0.000	0.000
13.77	0.000	0.000	0.000
15.53	0.000	0.000	0.159
20.51	0.003	0.000	0.000
23.54	0.000	0.000	0.000
24.51	0.000	0.974	0.000
25.01	0.943	0.000	0.000
25.89	0.000	0.000	0.000
27.22	0.000	0.004	0.000
32.84	0.000	0.000	0.000
35.49	0.002	0.000	0.000
36.77	0.000	0.000	0.000
40.90	0.000	0.000	0.020
41.06	0.000	0.000	0.000
43.97	0.001	0.000	0.000
44.67	0.000	0.000	0.000
48.45	0.000	0.000	0.000
48.66	0.000	0.000	0.040
51.44	0.000	0.000	0.000
54.01	0.000	0.000	0.006
60.36	0.000	0.000	0.000
66.09	0.000	0.000	0.000
66.19	0.000	0.000	0.000
68.80	0.000	0.000	0.007
74.25	0.000	0.000	0.000
78.30	0.000	0.000	0.000
80.56	0.000	0.000	0.000
80.69	0.000	0.000	0.000
81.37	0.000	0.000	0.046
82.17	0.000	0.000	0.000
86.31	0.000	0.000	0.000
89.52	0.000	0.000	0.006
95.39	0.000	0.000	0.000
97.21	0.000	0.000	0.000

Table 3.9.4-25
Side Heat Shield Modal Participating Mass Ratios
(2 Sheets)

Frequency (Hz)	Participating Mass Ratio		
	X-Direction	Y-Direction	Z-Direction
3.97	0.684	0.000	0.000
4.51	0.154	0.000	0.000
6.57	0.006	0.000	0.000
7.42	0.004	0.000	0.000
7.69	0.000	0.000	0.000
9.21	0.000	0.000	0.000
10.43	0.010	0.000	0.000
15.53	0.000	0.000	0.000
16.55	0.000	0.001	0.000
16.74	0.042	0.000	0.000
17.39	0.000	0.000	0.000
17.78	0.018	0.000	0.001
19.63	0.000	0.001	0.000
22.45	0.000	0.000	0.000
24.59	0.001	0.000	0.000
26.88	0.000	0.000	0.000
29.15	0.000	0.000	0.000
29.75	0.001	0.000	0.001
30.11	0.004	0.000	0.000
32.69	0.016	0.000	0.002
33.60	0.000	0.002	0.000
36.04	0.000	0.000	0.000
38.72	0.014	0.000	0.001
39.05	0.000	0.000	0.000
42.87	0.000	0.000	0.000
43.01	0.000	0.000	0.000
44.44	0.000	0.000	0.000
46.77	0.001	0.000	0.000
48.98	0.001	0.000	0.001
49.35	0.000	0.009	0.000
50.17	0.003	0.000	0.000
53.29	0.005	0.000	0.001
55.11	0.000	0.018	0.000
56.77	0.000	0.000	0.004
59.53	0.000	0.000	0.034
61.20	0.000	0.096	0.000

Table 3.9.4-25
Side Heat Shield Modal Participating Mass Ratios
(2 Sheets)

Frequency (Hz)	Participating Mass Ratio		
	X-Direction	Y-Direction	Z-Direction
64.18	0.000	0.000	0.179
64.44	0.000	0.001	0.000
65.87	0.000	0.000	0.000
66.19	0.001	0.000	0.425
67.23	0.000	0.509	0.000
68.47	0.002	0.000	0.255
70.35	0.000	0.326	0.000
71.92	0.000	0.000	0.009
74.26	0.000	0.001	0.000
75.55	0.000	0.000	0.059
76.08	0.000	0.002	0.000
79.42	0.000	0.000	0.000
81.57	0.002	0.000	0.015
83.62	0.000	0.018	0.000
83.79	0.000	0.000	0.001
86.33	0.001	0.000	0.001
88.01	0.000	0.001	0.000
91.46	0.000	0.002	0.000
92.25	0.000	0.000	0.000
92.56	0.000	0.000	0.000
93.78	0.000	0.001	0.000
96.86	0.003	0.000	0.001
97.14	0.000	0.000	0.000

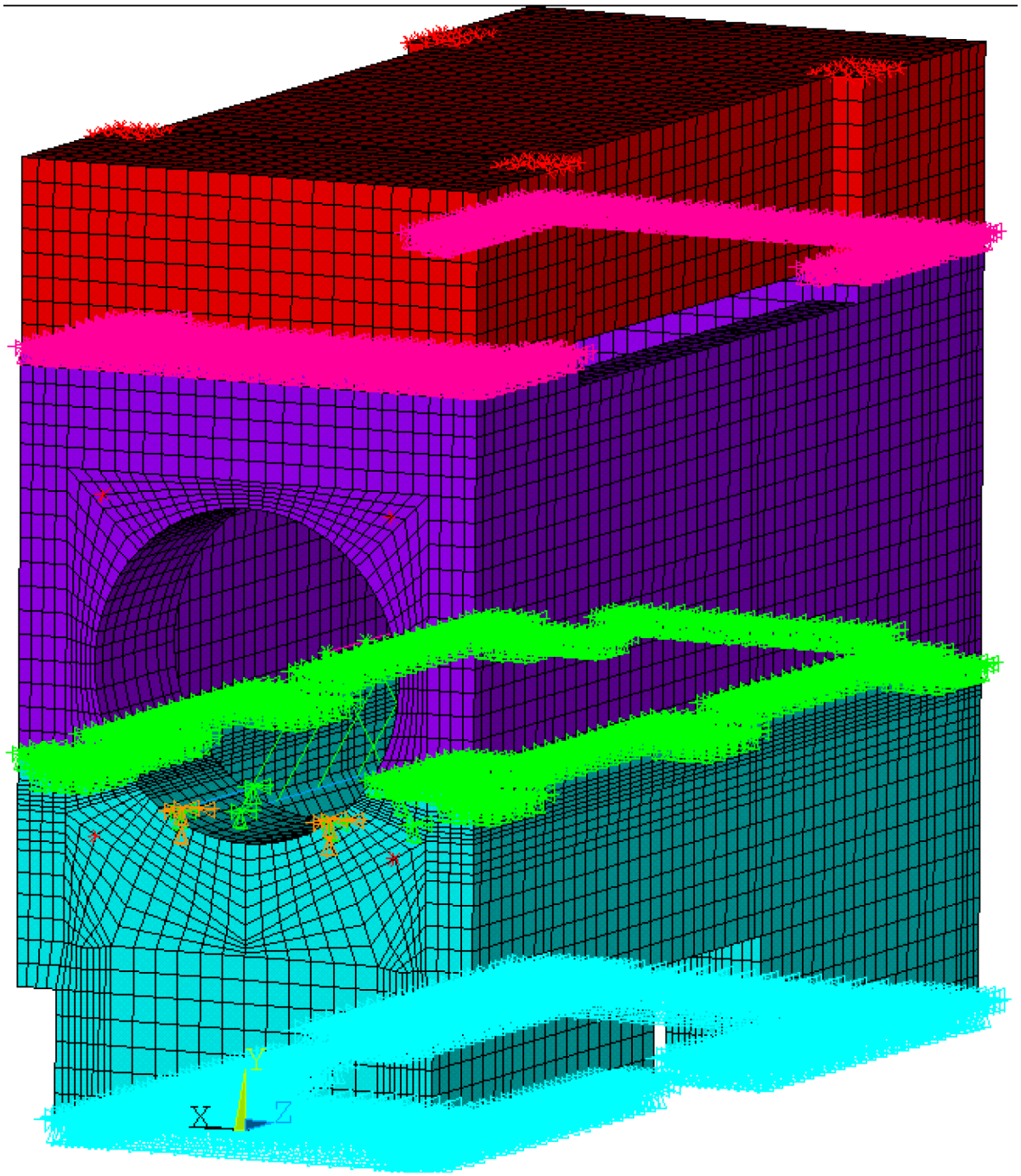

Figure 3.9.4-1
Analytical Model of EOS-HSM for Mechanical Load Analysis

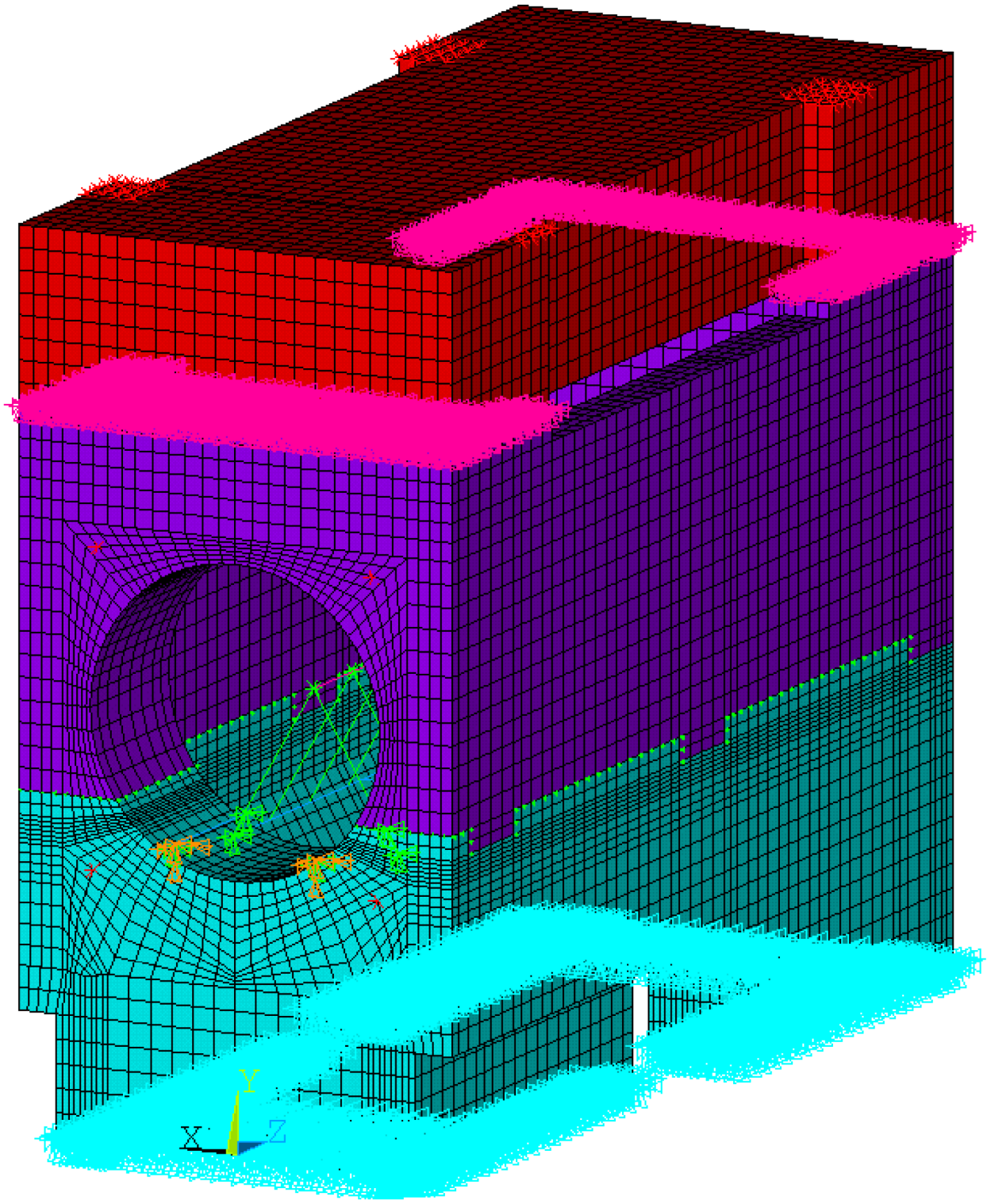

Figure 3.9.4-2
Analytical Model of EOS-HSMS for Mechanical Load Analysis
(Node to Node Contact at Segment Joint interface)

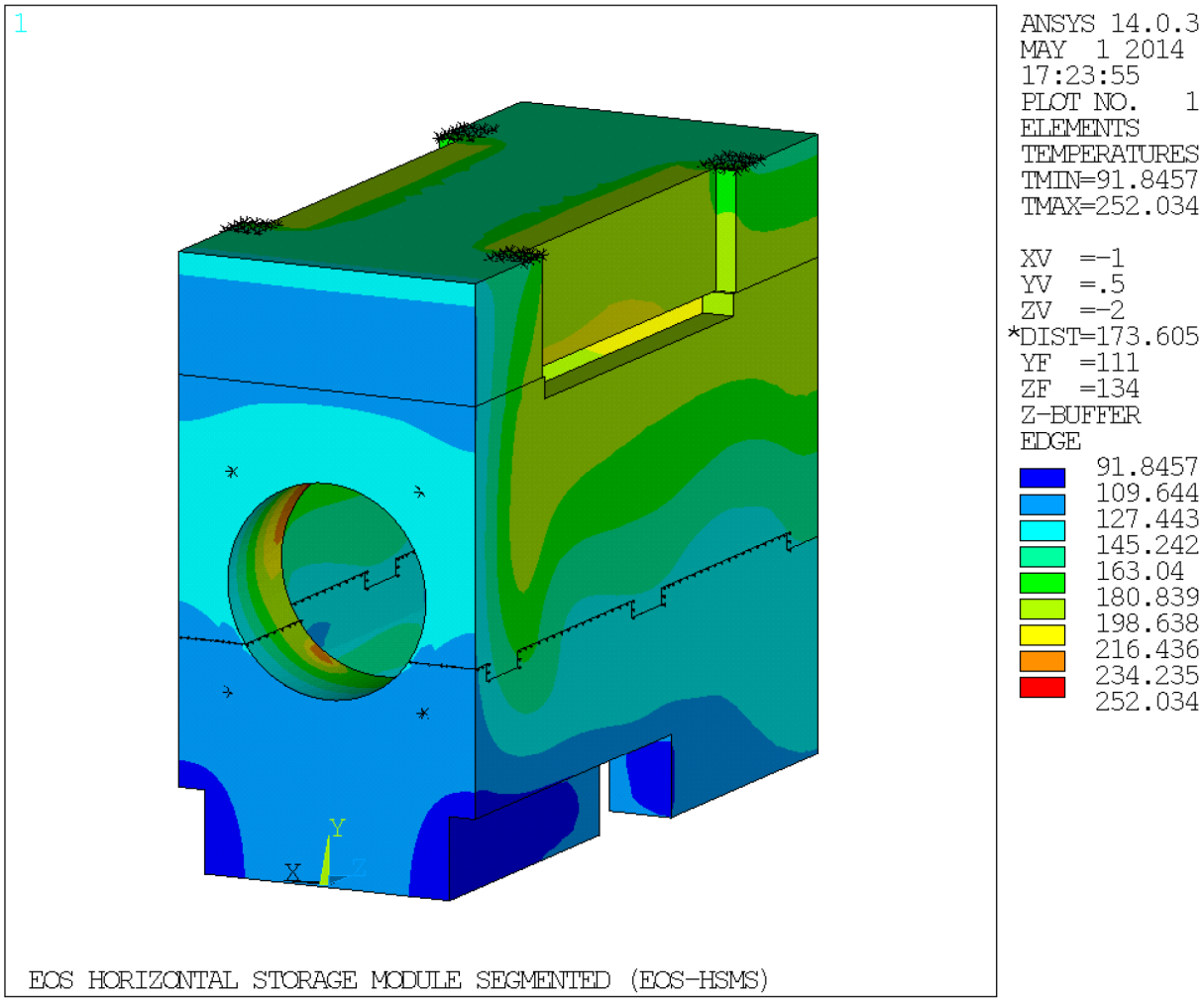

Figure 3.9.4-3
Temperature distribution of EOS-HSMS for Normal Thermal Hot Condition

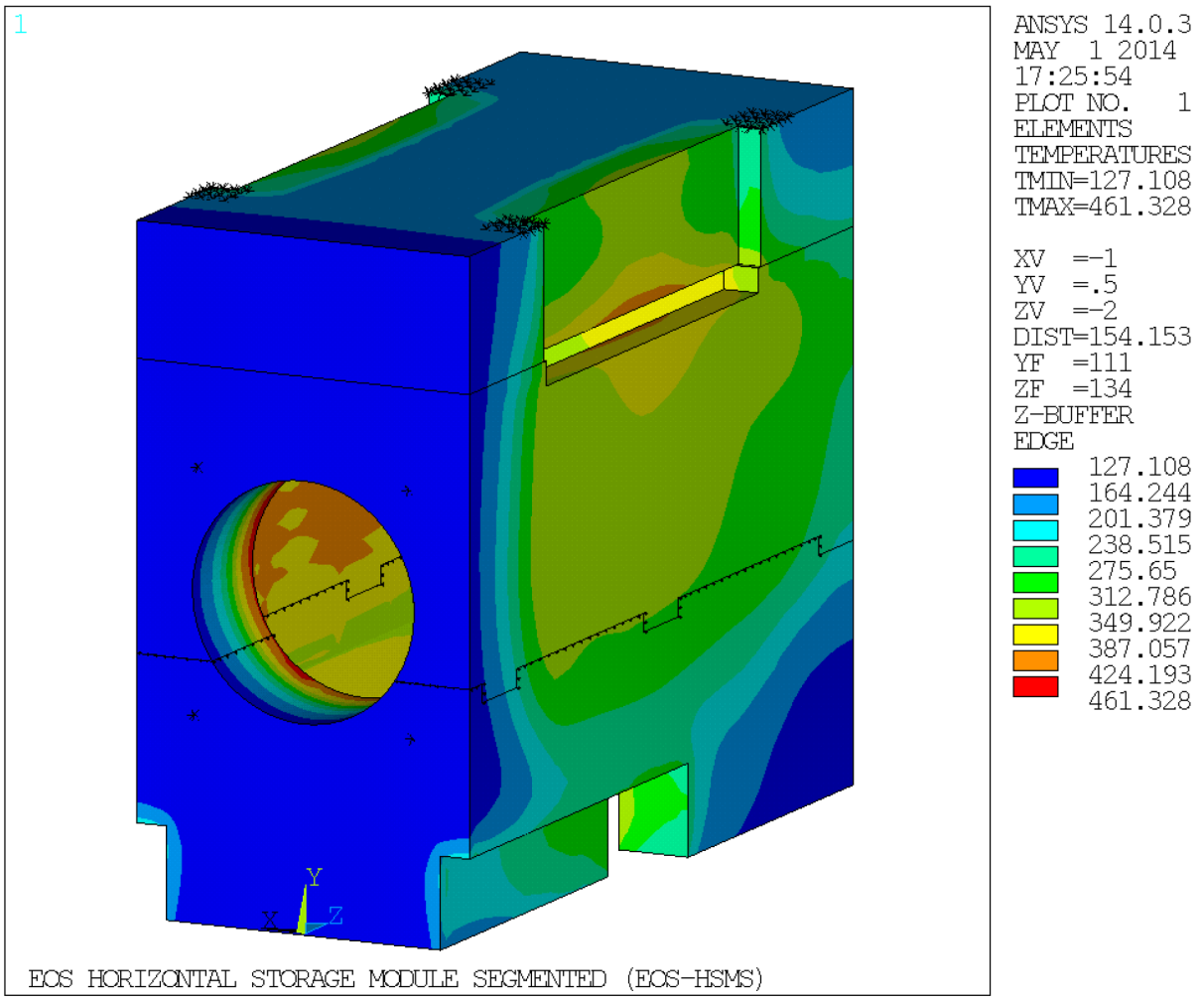

Figure 3.9.4-4
Temperature distribution of EOS-HSMS for Blocked Vent Accident Thermal Condition

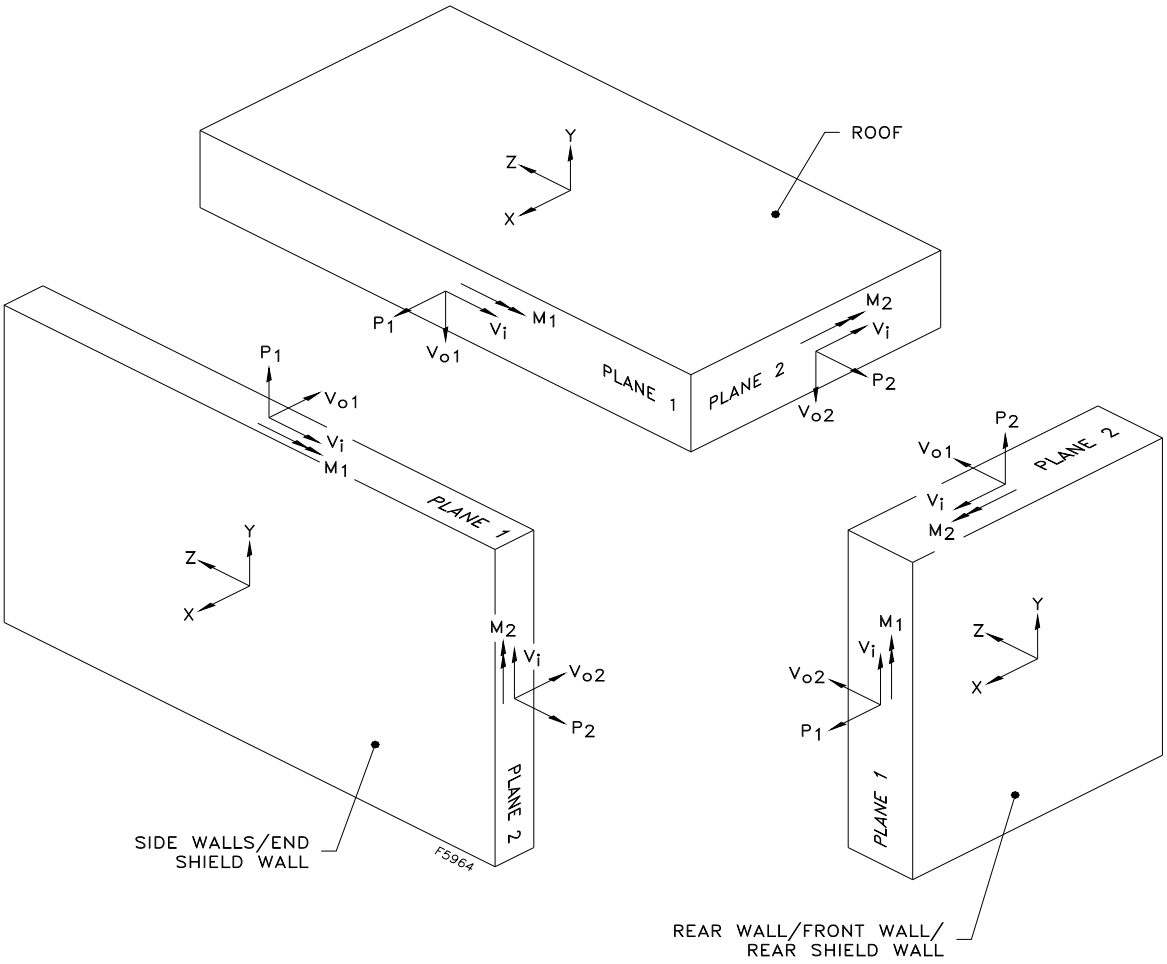

Figure 3.9.4-5
Symbolic Notation of Forces and Moments of EOS-HSM Concrete Components

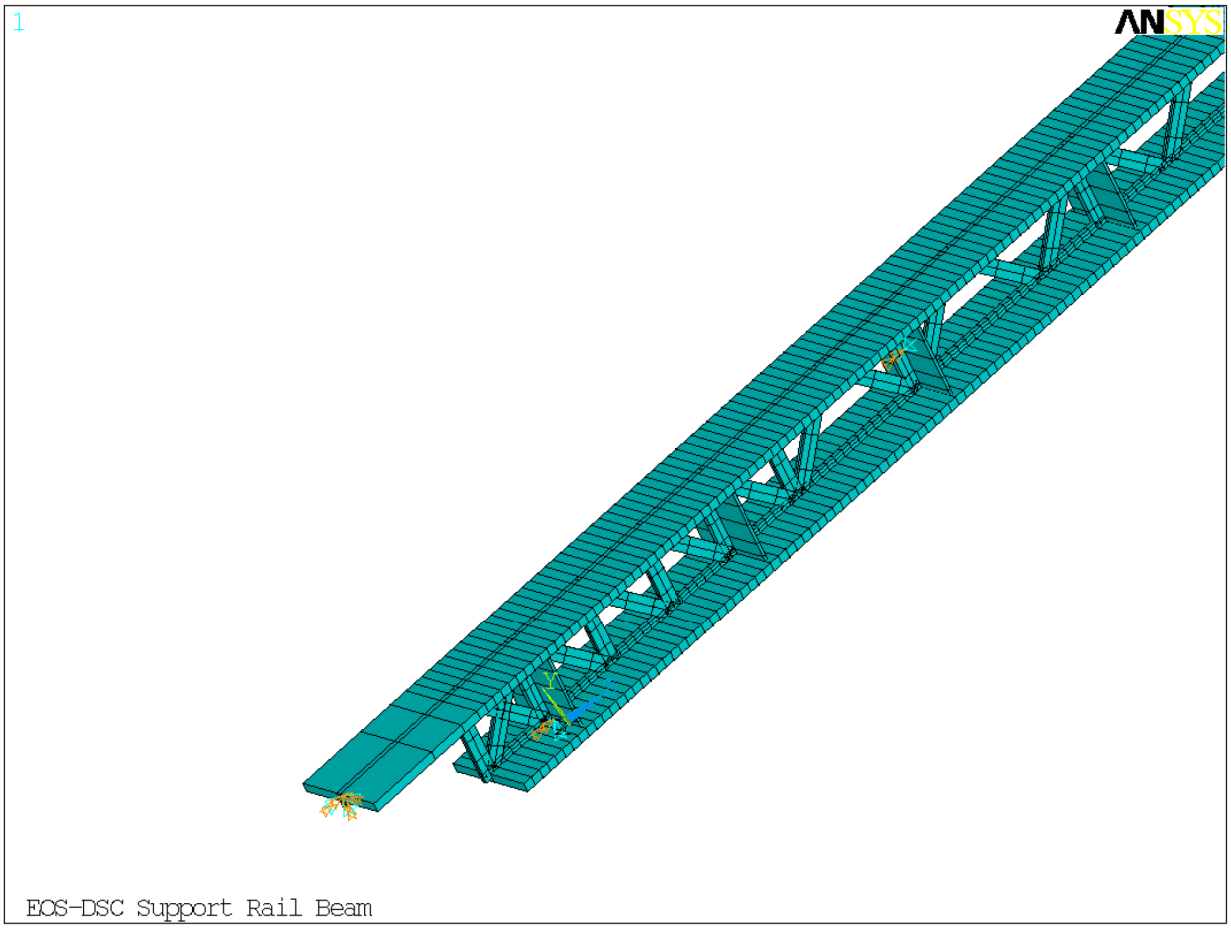

Figure 3.9.4-6
Analytical Model of the W12x136 DSC Main Support Beam with Stiffeners and Open Web

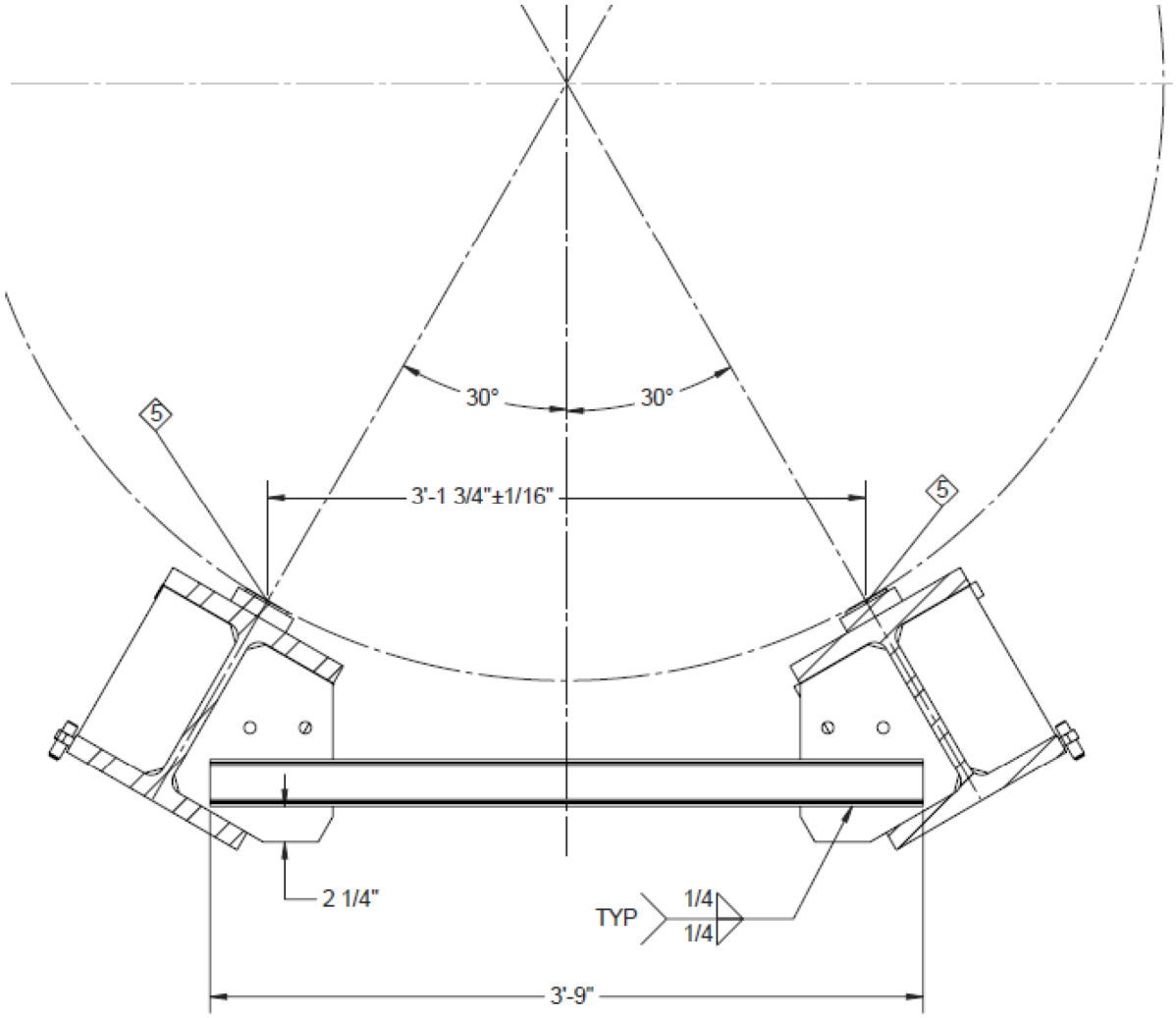

Figure 3.9.4-7
Components of DSC Support Structure

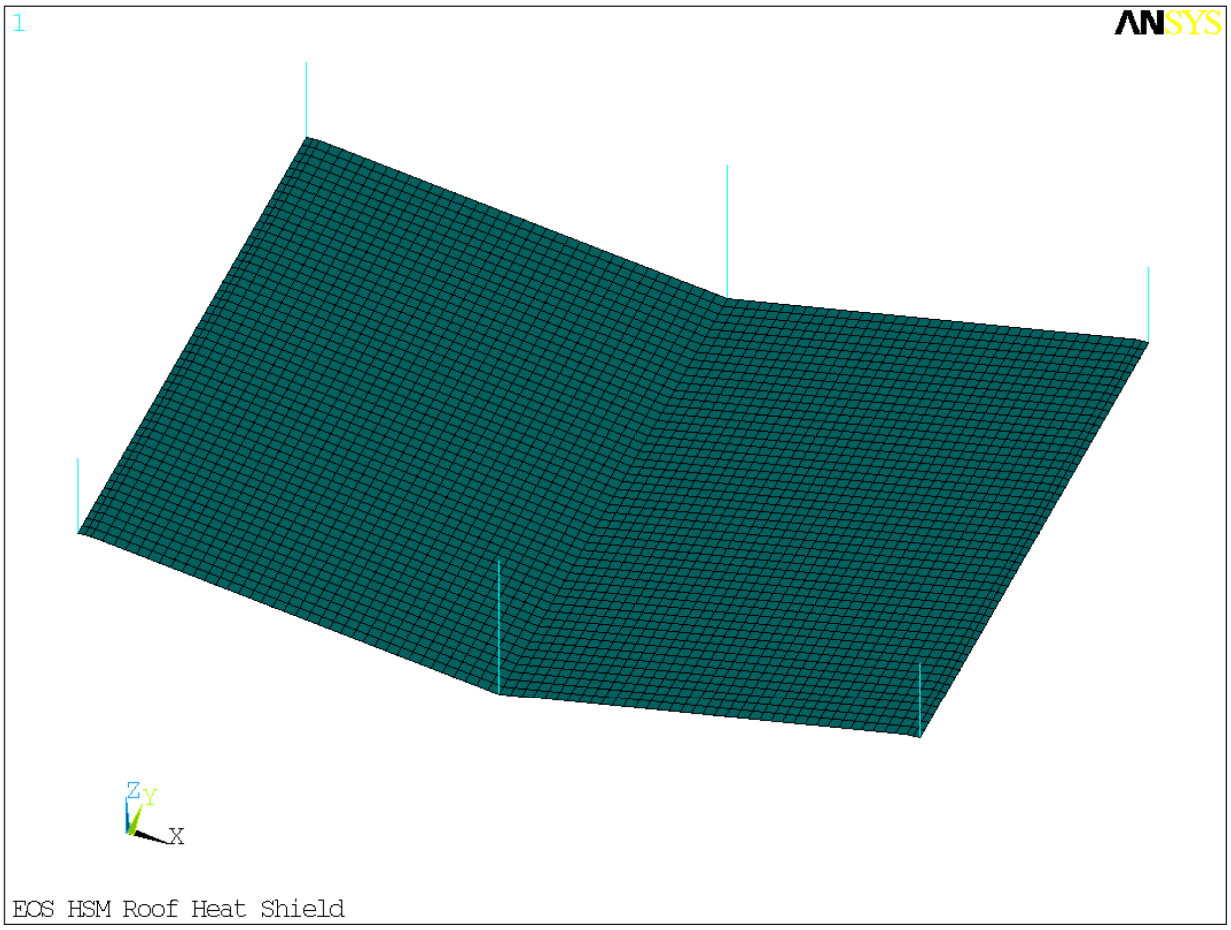

Figure 3.9.4-8
Analytical Model of Coupled Roof Heat Shield and Connection Studs

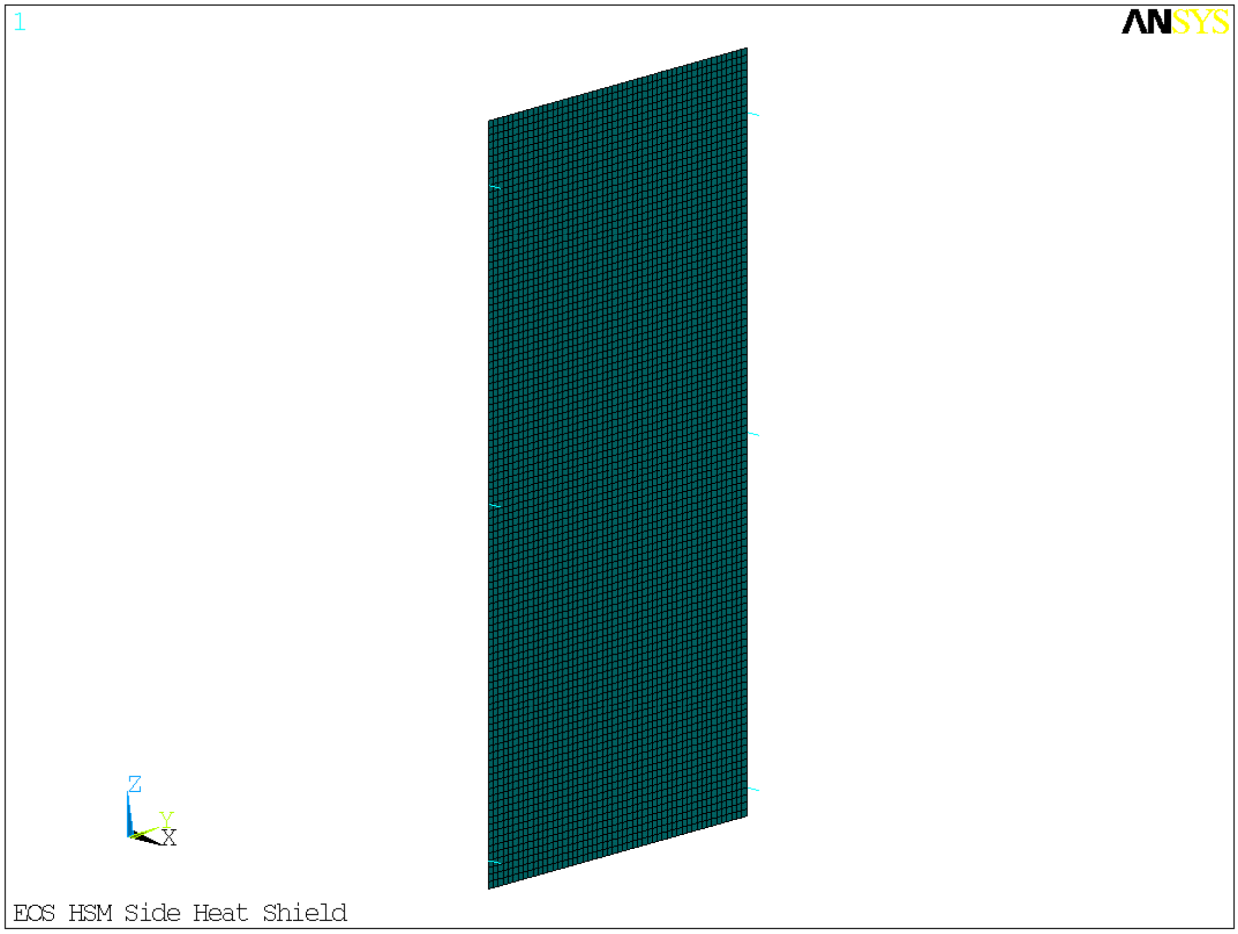

Figure 3.9.4-9
Analytical Model of Coupled Side Heat Shield and Connection Studs

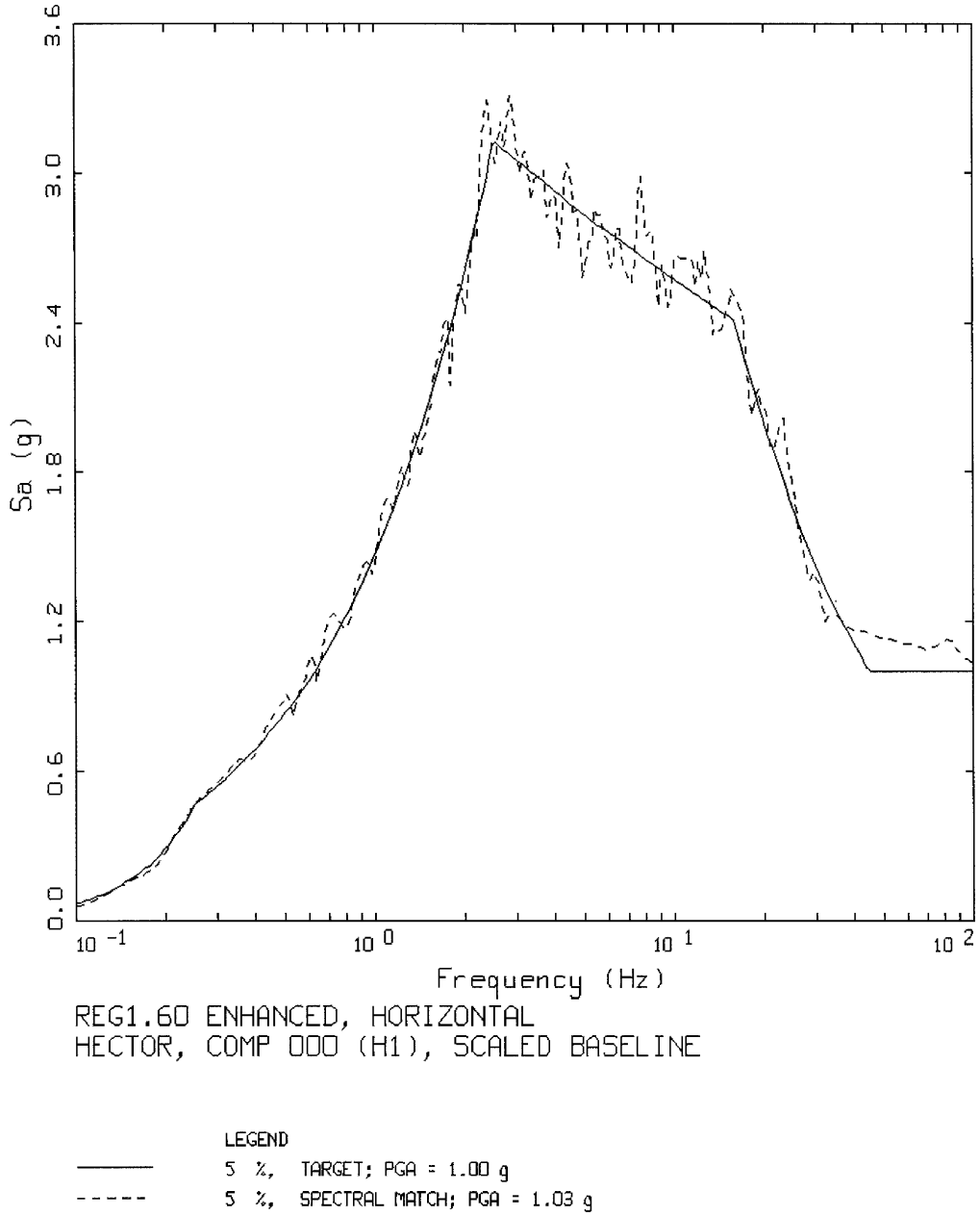

Figure 3.9.4-10
Horizontal Target and 5% Spectral Match (Horizontal 1, Hector Mine Earthquake)

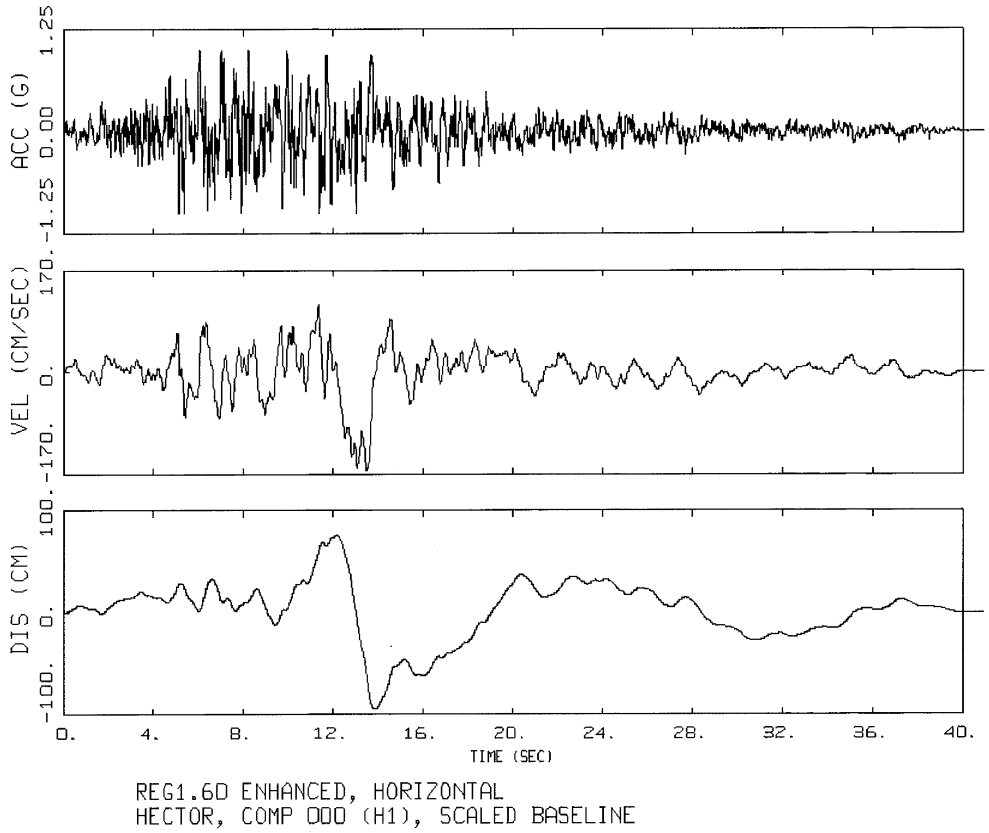

Figure 3.9.4-11
Baseline Corrected Acceleration, Velocity and Displacement Time Histories
(Horizontal 1, Hector Mine Earthquake)

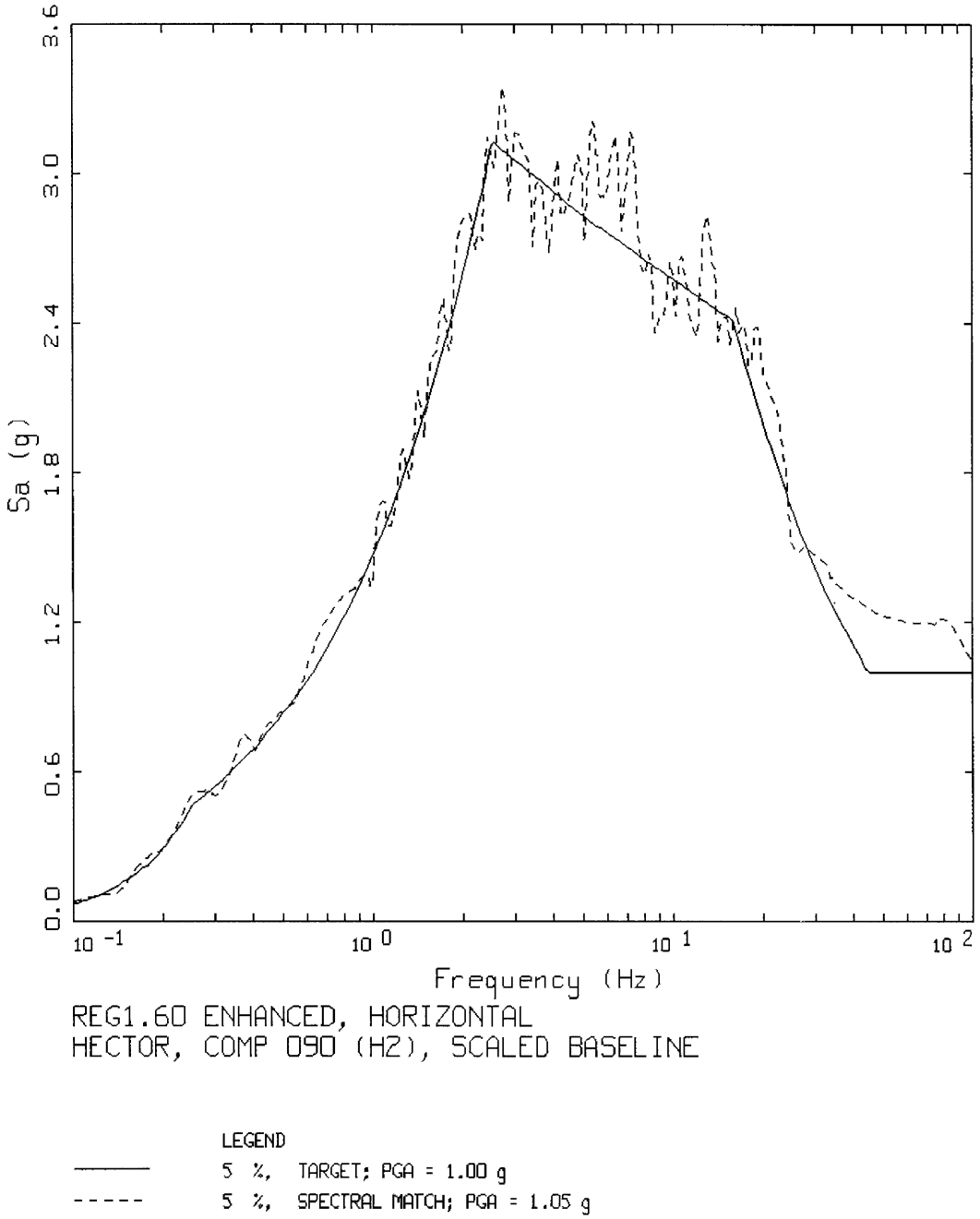

Figure 3.9.4-12
Horizontal Target and 5% Spectral Match (Horizontal 2, Hector Mine Earthquake)

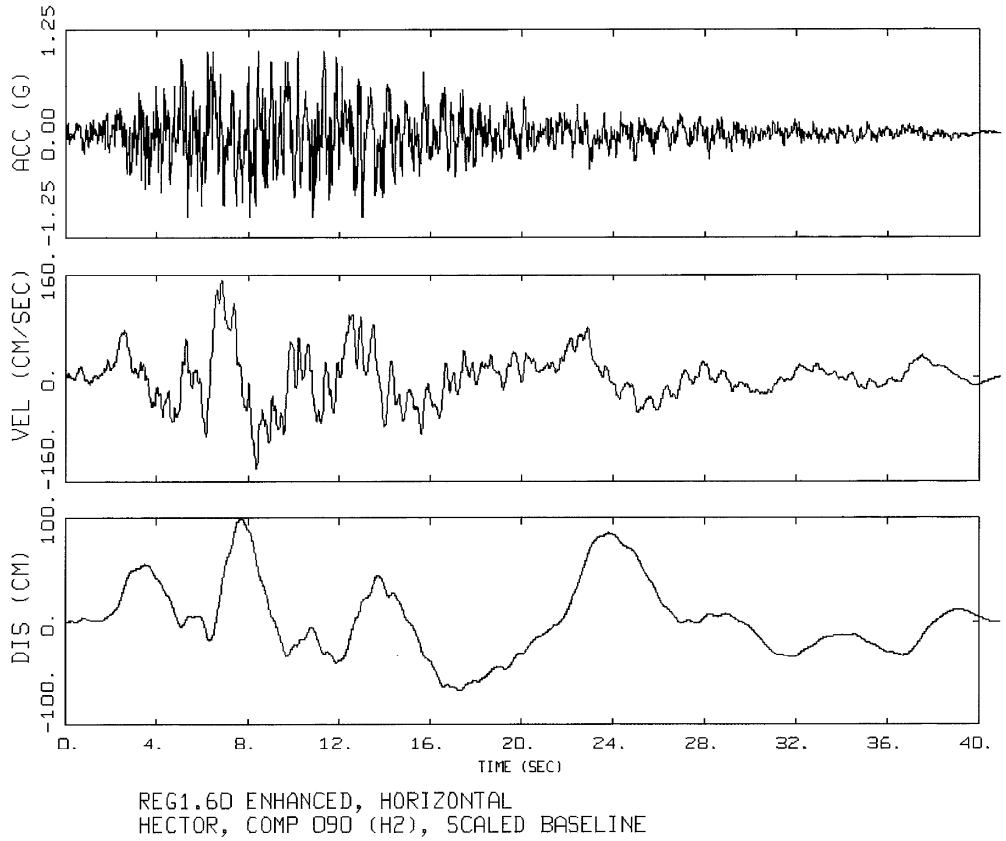

Figure 3.9.4-13
Baseline Corrected Acceleration, Velocity and Displacement Time Histories (Horizontal 2, Hector Mine Earthquake)

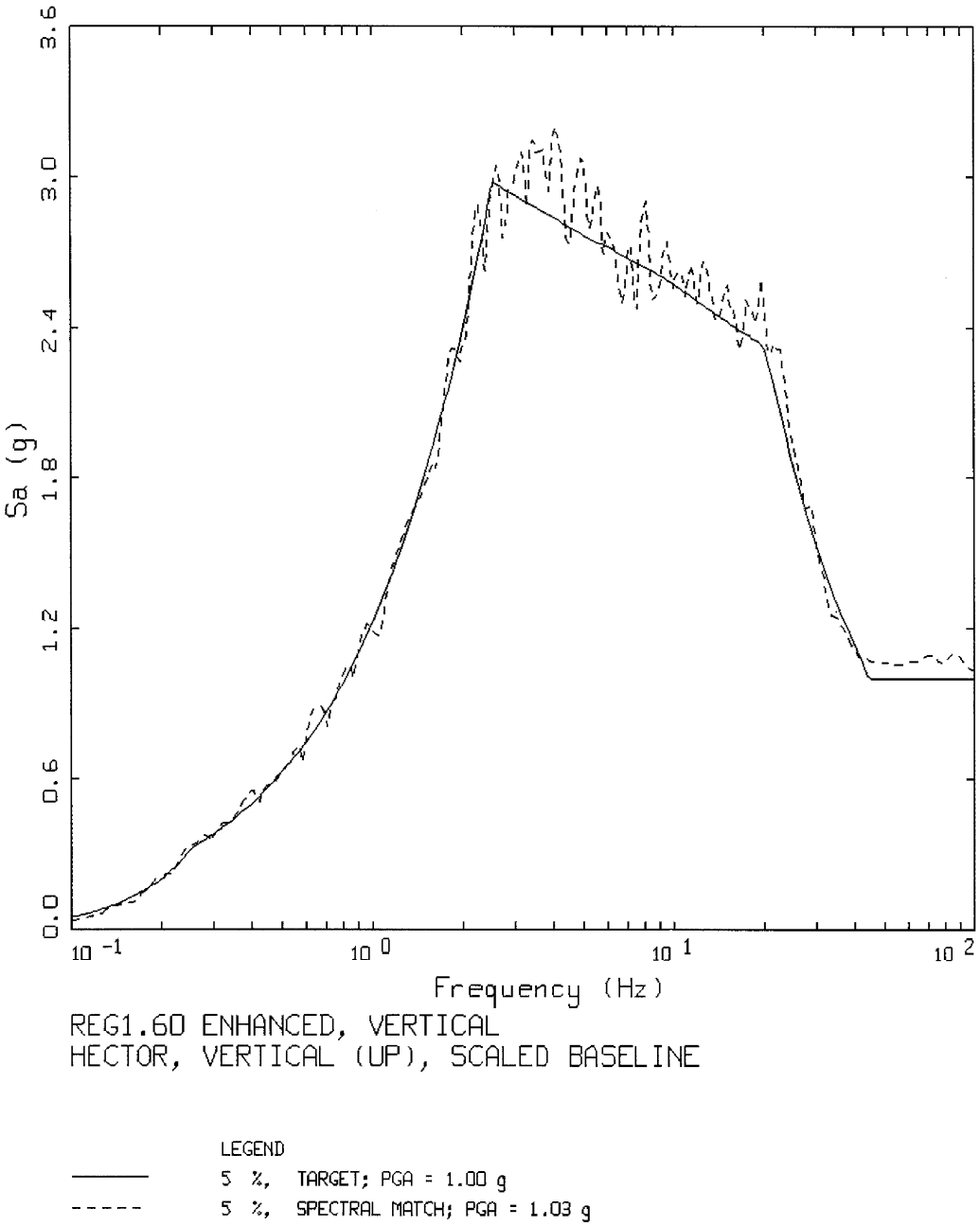

Figure 3.9.4-14
Vertical Target and 5% Spectral Match (Vertical Up, Hector Mine Earthquake)

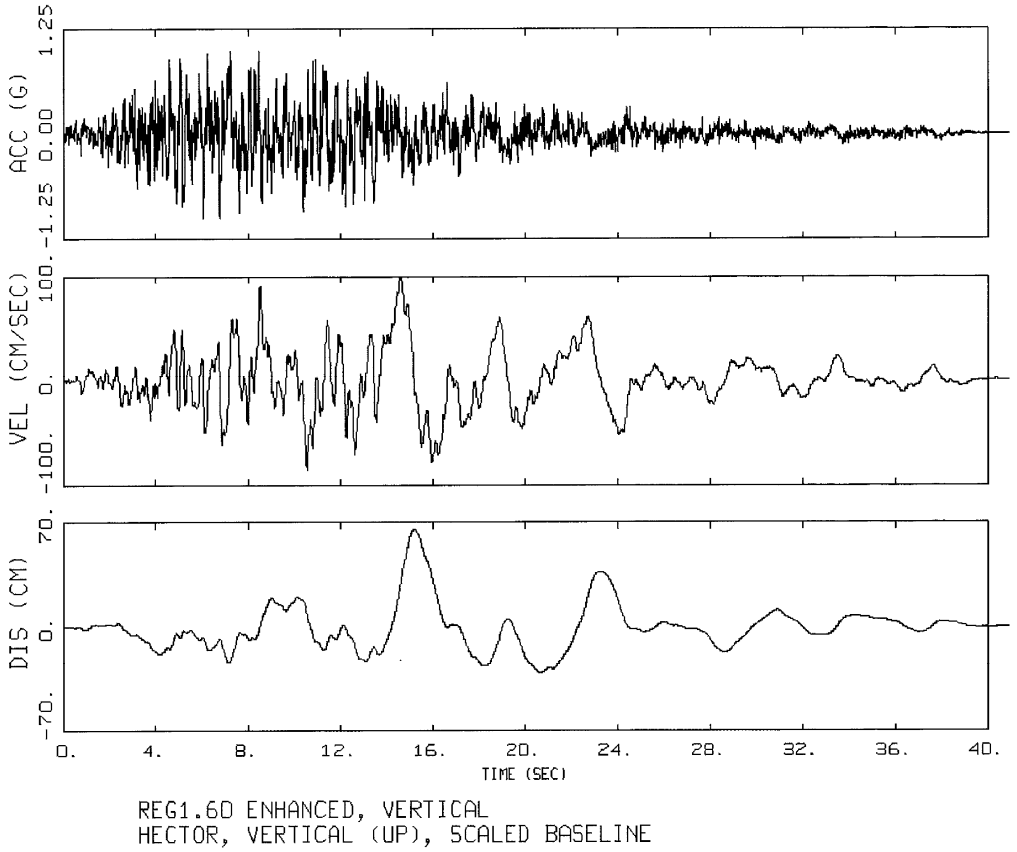

Figure 3.9.4-15
Baseline Corrected Acceleration, Velocity and Displacement Time Histories
(Vertical Up, Hector Mine Earthquake)

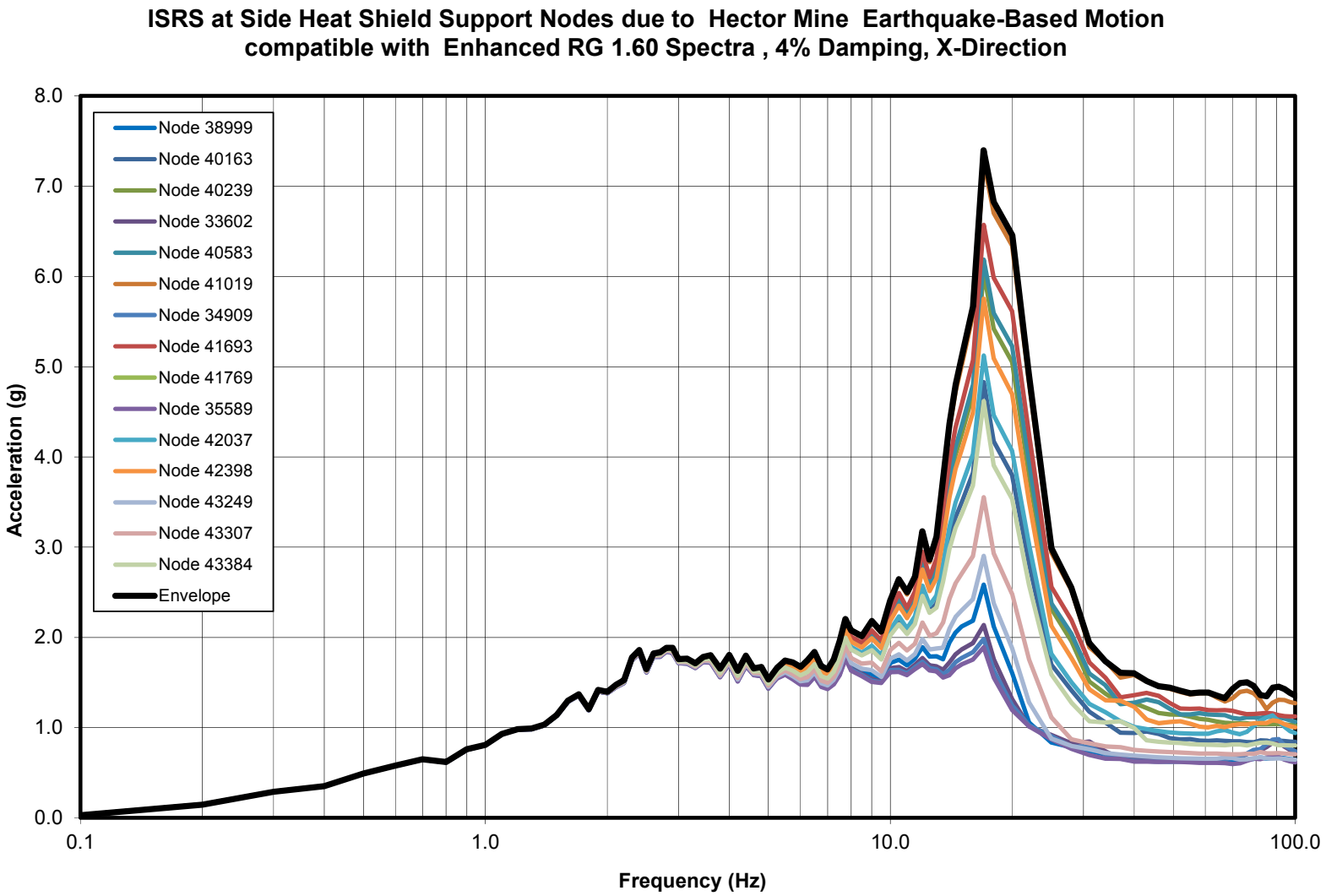

Figure 3.9.4-16
ISRS at Side Heat Shield Support Nodes due to Hector Mine Earthquake-Based Motion compatible with Enhanced RG 1.60 Spectra, 4% Damping, X-Direction

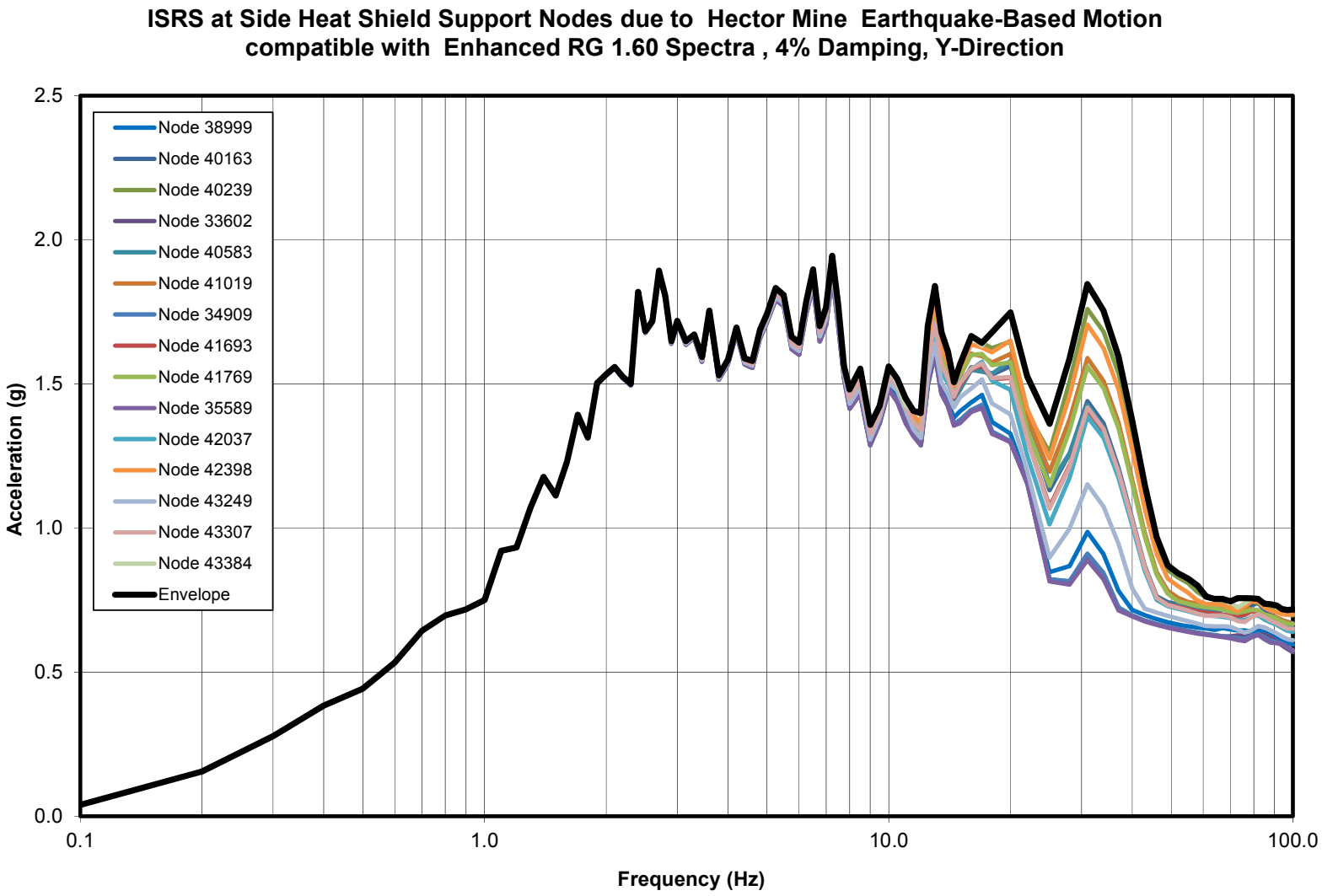

Figure 3.9.4-17
ISRS at Side Heat Shield Support Nodes due to Hector Mine Earthquake-Based Motion compatible with Enhanced RG 1.60 Spectra, 4% Damping, Y-Direction

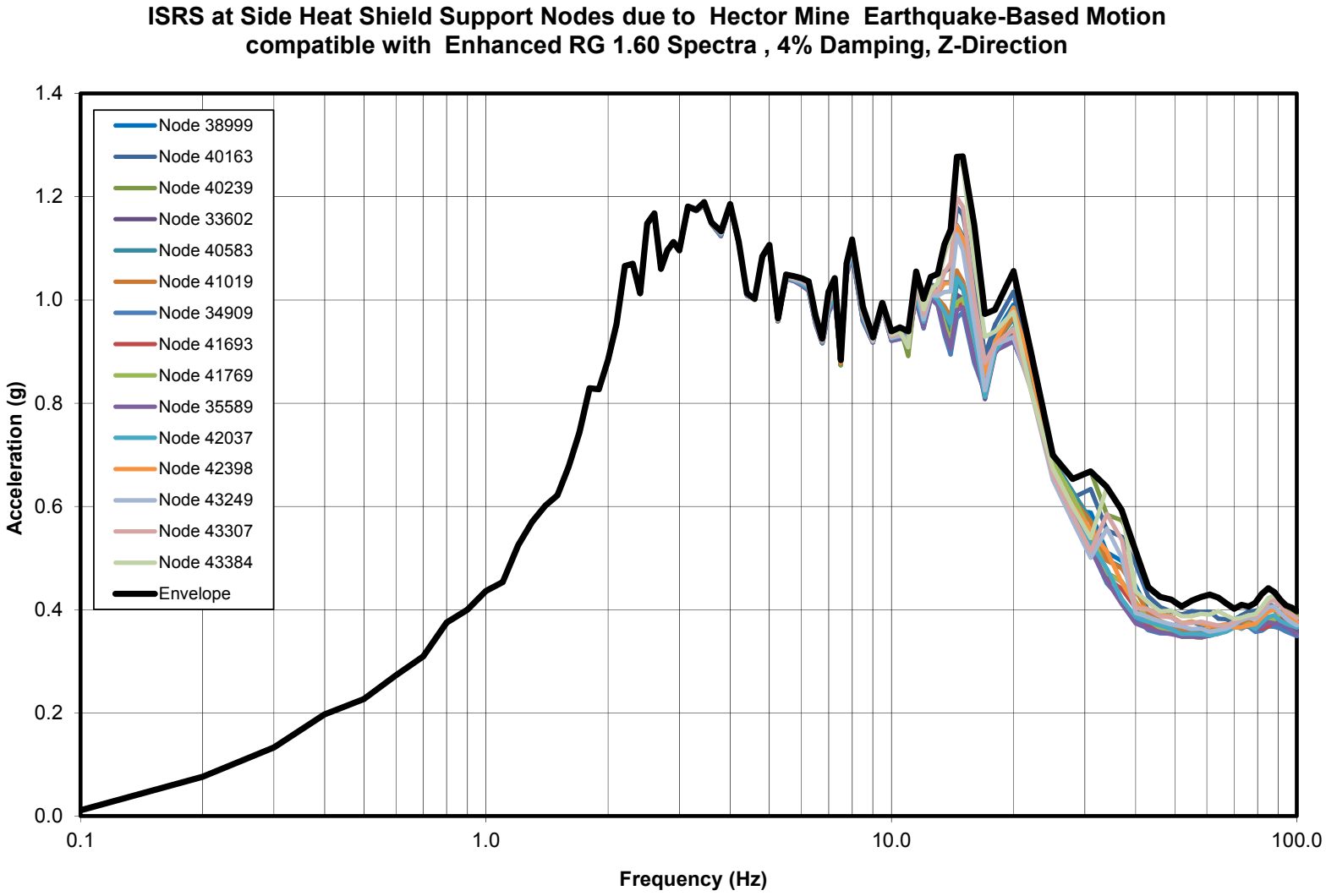

Figure 3.9.4-18
ISRS at Side Heat Shield Support Nodes due to Hector Mine Earthquake-Based Motion compatible with Enhanced RG 1.60 Spectra, 4% Damping, Z-Direction

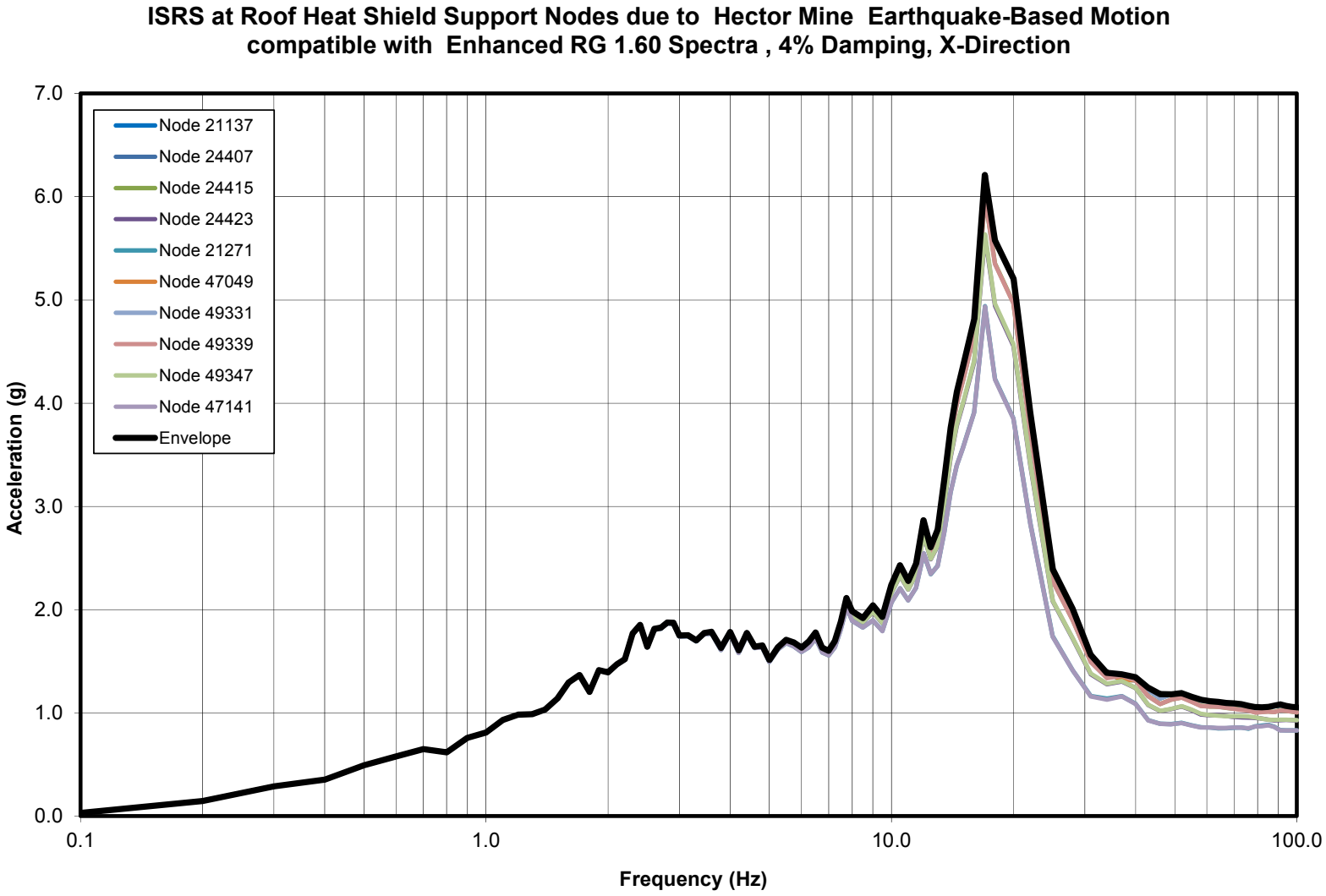

Figure 3.9.4-19
ISRS at Roof Heat Shield Support Nodes due to Hector Mine Earthquake-Based Motion compatible with Enhanced RG 1.60 Spectra, 4% Damping, X-Direction

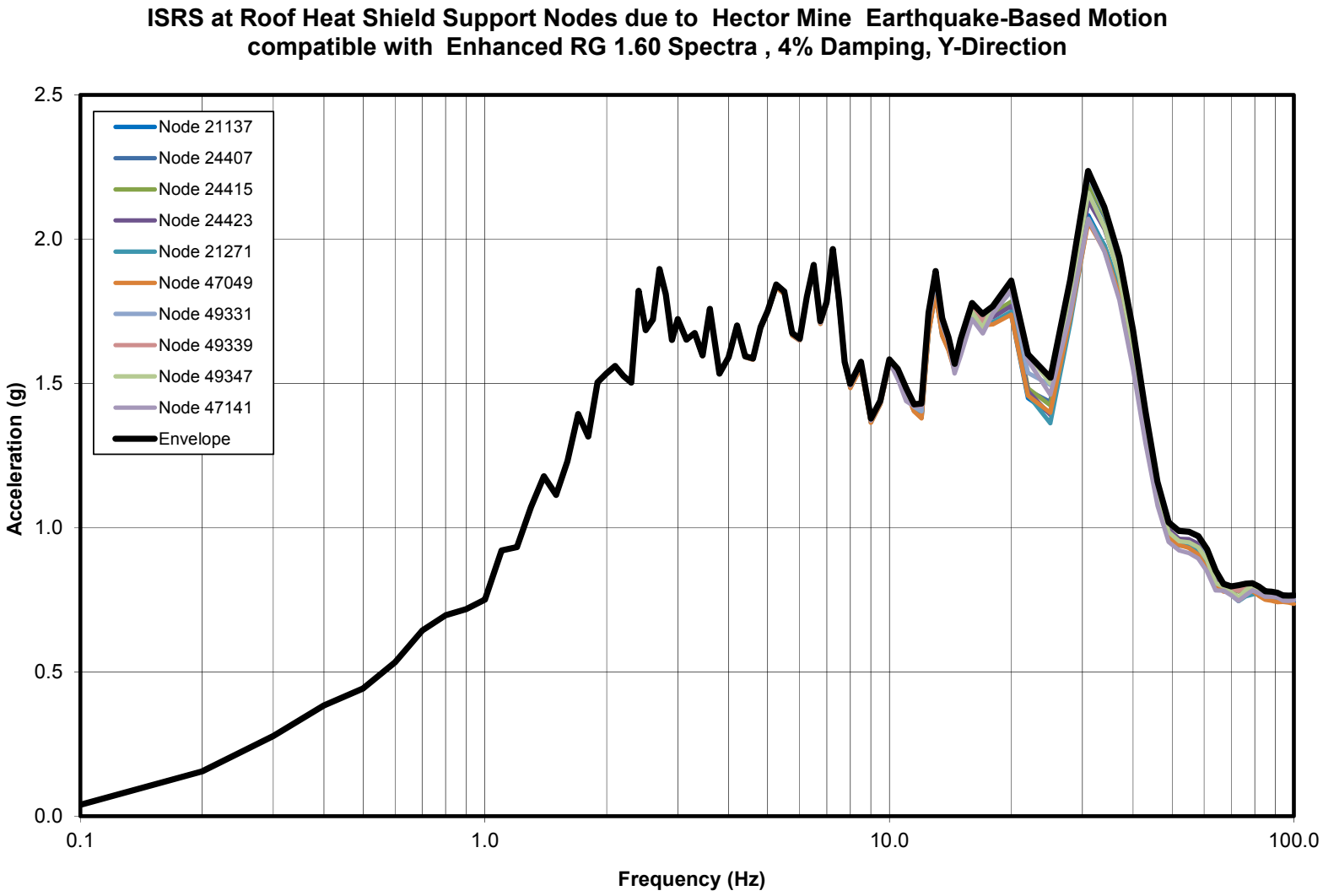

Figure 3.9.4-20
ISRS at Roof Heat Shield Support Nodes due to Hector Mine Earthquake-Based Motion compatible with Enhanced RG 1.60 Spectra, 4% Damping, Y-Direction

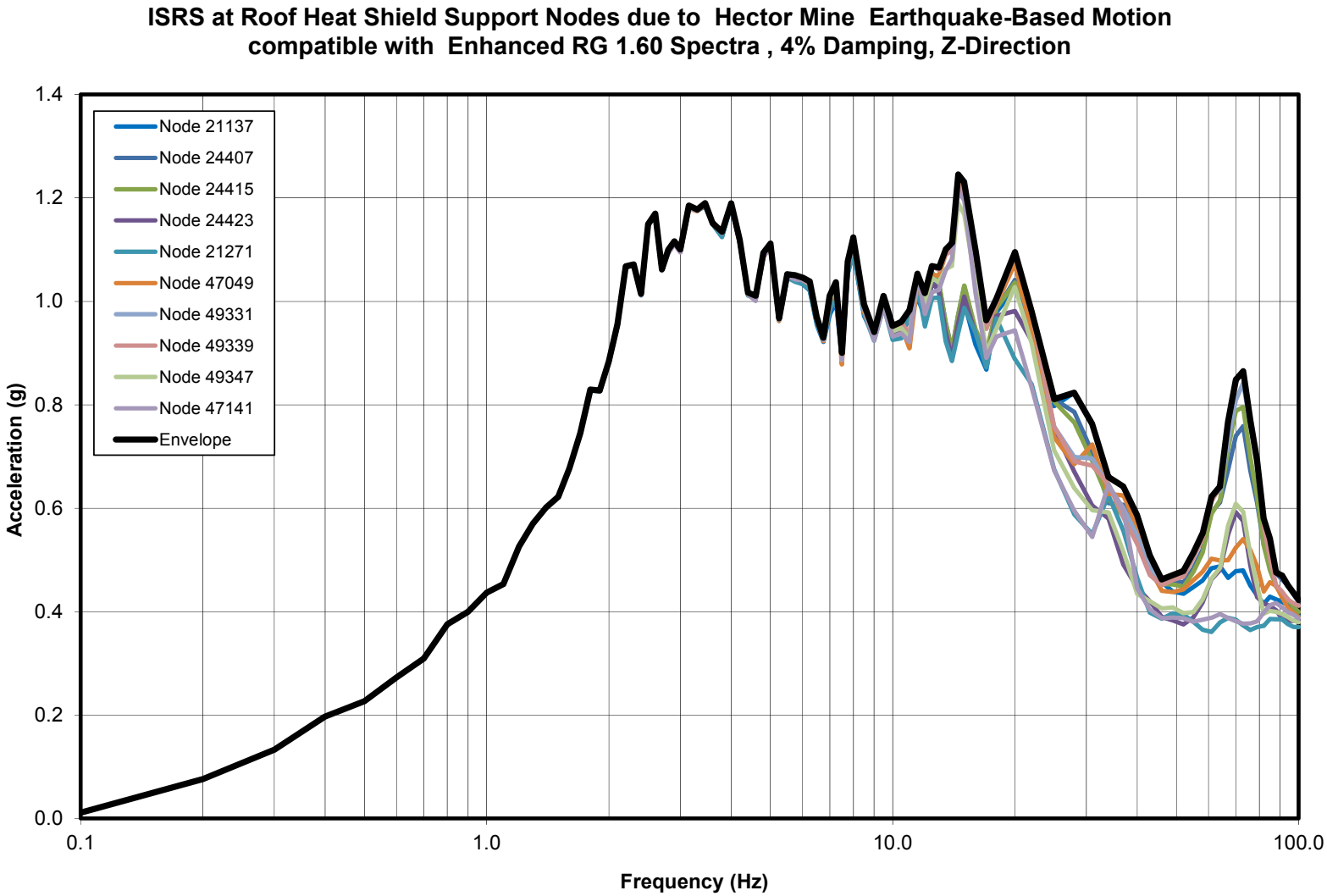

Figure 3.9.4-21
ISRS at Roof Heat Shield Support Nodes due to Hector Mine Earthquake-Based Motion compatible with Enhanced RG 1.60 Spectra, 4% Damping, Z-Direction